

BLACK HOLE EMERGENCE IN SUPERNOVAE

SHMUEL BALBERG¹, LUCA ZAMPIERI^{1,2} AND STUART L. SHAPIRO^{1,3}

To appear in the Astrophysical Journal, 540, 2000 September 10

ABSTRACT

If a black hole formed in a core-collapse supernova is accreting material from the base of the envelope, the accretion luminosity could be observable in the supernova light curve. Here we continue the study of matter fall back onto a black hole in the wake of a supernova and examine realistic supernovae models which allow for an early emergence of the accretion luminosity. Such cases may provide a direct *observational* identification of the black hole formed in the aftermath of the explosion. Our approach combines analytic estimates and fully relativistic, radiation-hydrodynamic numerical computations. We employ a numerical hydrodynamical scaling technique to accommodate the diverse range of dynamical time scales in a single simulation. We find that while in typical Type II supernovae heating by radioactive decays dominates the late-time light curve, low-energy explosions of more massive stars should provide an important exception where the accretion luminosity will emerge while it is still relatively large. Our main focus is on the only current candidate for such an observation, the very unusual SN1997D. Due to the low energy of the explosion and the very small ($2 \times 10^{-3} M_{\odot}$) inferred mass of ^{56}Co in the ejected envelope, we find that accretion should become the dominant source of its luminosity during the year 2000. The total luminosity at emergence is expected to lie in the range $0.5 - 3 \times 10^{36}$ ergs s^{-1} , potentially detectable with HST. We also discuss the more favorable case of explosions which eject negligible amounts of radioactive isotopes and find that the black hole is likely to emerge a few tens of days after the explosion, with a luminosity of $\sim 10^{37}$ ergs s^{-1} .

Subject headings: accretion, accretion disks — black holes — methods: numerical — supernovae: general — supernovae: individual (SN1997D)

1. INTRODUCTION

Core-collapse supernovae mark the death of a massive star and the birth of a compact remnant. Theory suggests that the remnant can be either a neutron star or a black hole, depending on the character of the progenitor and the details of the explosion. Radio pulsar emission has allowed to compile a variety of observational evidence associating neutron stars with sites of known supernovae, but similar evidence for a black hole - supernova connection is still mostly unavailable. Interestingly, indirect evidence that the black hole candidate in the X-ray binary system GRO J1655-40 was formed in a supernova explosion has recently been reported by Israelian et al. (1999). The inference is based on detection of high abundances of nitrogen and oxygen on the surface of the companion, which has too low a mass to have produced them by thermonuclear burning, hence indicating that they were deposited there by the supernova that created the black hole.

The formation of a compact object in a supernova can be inferred *directly* if the object causes an observable effect on the total luminosity which follows the explosion – i.e., the *light curve*. In particular, some material from the base of the expanding envelope may remain bound to the compact object and continuously fall back onto it, thus generating an accretion luminosity. Zampieri et al. (1998a) have recently performed a

self-consistent investigation of the accretion luminosity generated by spherically symmetric “fallback” of matter onto a black hole in the wake of a supernova. With the aid of a general-relativistic, radiation hydrodynamic Lagrangian code they showed that, at late times, the fallback evolves quasi-stationarily with the accretion luminosity obeying the analytic expression found by Blondin (1986) for steady state, spherical hypercritical accretion⁴. The accretion luminosity declines secularly with a time dependence of $t^{-25/18}$. This decay is driven by the decrease in the accretion rate due to the continuous expansion of the supernova envelope (Colpi, Shapiro & Wasserman 1996),

Such an accretion luminosity will produce a distinct signature on the total light curve if and when it becomes comparable to the output of other power sources, namely the initial internal energy of the envelope and decays of radioactive isotopes synthesized in the explosion. It is well established that the efficiency of converting spherical accretion onto a black hole into radiative luminosity may be quite low (Shapiro 1973; Blondin 1986; Wandel, Yahil & Milgrom 1986; Park 1990; Nobili, Turolla & Zampieri 1991; Zampieri, Miller & Turolla 1996), and, in general, the accretion luminosity will be undetectable in comparison with the luminosity generated by radioactive decays. This is particularly important when compared to the case of accretion onto a neutron star, which is expected

¹Department of Physics, Loomis Laboratory of Physics, University of Illinois at Urbana-Champaign, 1110 West Green Street, Urbana, IL 61801-3080, sbalberg@astro.physics.uiuc.edu, shapiro@astro.physics.uiuc.edu

²Department of Physics, University of Padova, Via Marzolo 8, 35131 Padova, Italy, zampieri@pd.infn.it

³Department of Astronomy and National Center for Supercomputing Applications, University of Illinois at Urbana-Champaign, Urbana, IL 61801

⁴We use the term “hypercritical” to describe an accretion rate \dot{M} that largely exceeds the Eddington limit for the accreting object, i.e., $\dot{M} \gg \dot{M}_{Edd} \equiv L_{Edd}/c^2$. The actual luminosity that arises would still be sub-Eddington if the efficiency of converting energy into radiative luminosity is low enough.

to be far more efficient in generating an accretion luminosity. For the last decade this distinction has been specifically applied to the case of SN1987A: Chevalier (1989) and Houck & Chevalier (1991) found that accretion onto a newly formed neutron star in SN1987A would generate an accretion luminosity at the Eddington-rate ($\gtrsim 10^{38}$ ergs s^{-1}) within a few months after the explosion, and the luminosity would persist at this rate for several years⁵. The proximity of SN1987A has allowed observations to follow the light curve for over 3000 days (to a present luminosity of $\sim 10^{36}$ ergs s^{-1}), and the light curve has been completely consistent with heating by decays of ^{56}Co , ^{57}Co and ^{44}Ti . The absence of any evidence for accretion luminosity in the case of SN1987A has been used to argue that the compact remnant in SN1987A is a low mass black hole, implying significant consequences regarding the nuclear equation of state (Bethe & Brown, 1995). It has also been argued, however, that this absence could still be consistent with a weakly magnetized neutron star, if the accretion flow has become dynamically unstable (Fryer, Colgate & Pinto 1999).

A positive indication of the presence of a black hole would be an actual detection of the accretion luminosity. The power-law time dependence would make the accretion luminosity easily discernible from luminosity generated by radioactive heating, which decreases exponentially with time. Furthermore, the difference in the time dependence implies that the accretion luminosity *must* eventually become dominant over radioactive decays, so in principle, the black hole always “emerges” in supernovae light curves. However, the potential for observation is usually quite slim: for example, Zampieri et al. (1998a) estimated that if a low mass black hole was formed in SN1987A, the accretion luminosity will not become dominant over that of heating by ^{44}Ti decays until ~ 900 years after the explosion, when the luminosity will have dropped to a mere 10^{32} ergs s^{-1} . The abundance of radioactive elements and the amount of fallback in SN1987A are rather typical of core collapse supernovae of low to intermediate mass progenitors ($12\text{--}25 M_{\odot}$) so that, if a black hole is formed, the “emergence” of the accretion luminosity occurs only at such late times and low luminosities that it is of no observational consequence.

An important exception may exist, however, in the explosions of more massive stars. In their survey of supernova explosions and nucleosynthesis, Woosley & Weaver (1995) find that more massive stars tend to produce more massive compact remnants: the original iron core is larger, leading to a more massive proto-neutron star and to larger amounts of fallback (see also Fryer 1999). Correspondingly, larger mass progenitors are more likely to produce black holes (as the remnant mass would be larger than the maximum mass of stable neutron stars), and to have larger amounts of material that remain bound to the black hole as a reservoir for late time fallback. Just as important, the final abundance of the key radioactive isotopes (^{56}Ni , ^{57}Ni and ^{44}Ti) in the expanding envelope is quite sensitive to the location of the cutoff that defines the material which settles on the black hole during the early stages (while the explosion is still proceeding). For the more massive progenitors the cutoff is further out, and since the radioactive elements are synthesized in the innermost layers above the proto-neutron star, the total mass of these elements in the ejected envelopes of higher mass stars can be significantly smaller than in “standard” supernovae. In fact, progenitor of masses in the range $30\text{--}40 M_{\odot}$, are expected to be practically free of radioactive elements that can

power the bolometric light curve (Woosley & Weaver, 1995). For such stars, black hole accretion luminosity should emerge immediately after the decay of the recombination peak (tens of days after the explosions), while it is still relatively powerful, and hence potentially observable.

Naturally, the more massive stars are a small minority in the stellar population, as are their explosions among core collapse supernovae. However, one recent supernova, SN1997D in NGC 1536 (deMello & Benetti, 1997), may present a border-line candidate for a direct detection of black hole emergence. Its observed light curve indicates that the total mass of ^{56}Co (the daughter of ^{56}Ni) in the envelope is only $\sim 2 \times 10^{-3} M_{\odot}$, a factor of ~ 35 lower than SN1987A. By analyzing the light curve and spectra, Turatto et al. (1998) suggested that SN1997D was a low energy ($E_{\text{tot}} \sim 4 \times 10^{50}$ ergs) explosion of a $26 M_{\odot}$ star. The expected mass of the remnant is about $3 M_{\odot}$ (formed by a $1.2 M_{\odot}$ early fallback on a $1.8 M_{\odot}$ collapsed core), hence most likely a black hole. Based on the inferred average properties of the material available for late time fallback and on the late time behavior of the accretion luminosity found by Zampieri et al. (1998a), Zampieri, Shapiro & Colpi (1998b) estimated that accretion luminosity will emerge in SN1997D in the optical band within *only a few years* after the explosion.

In this work we revisit the issue of black hole emergence in supernova due to spherically-symmetric late-time accretion. In particular, we investigate a more robust estimate for our “proto-type” case, SN1997D. We furnish revised analytic estimates and a detailed numerical investigation of the radiation-hydrodynamic evolution of the ejecta, incorporating the effects of a realistic chemical composition, opacities and radioactive heating on the accretion history and luminosity. The numerical study is based on an improved version of the radiation-hydrodynamic code used by Zampieri et al. (1998a), where the main modifications are the inclusion of realistic envelope composition and opacities (rather than pure hydrogen) and of heating by radioactive decays. We find that a $3 M_{\odot}$ black hole should emerge in the SN1997D light curve at about 1000-1500 days after the explosion – i.e., *during late 1999 and 2000* – when the total bolometric luminosity is $\sim 0.5\text{--}3 \times 10^{36}$ ergs s^{-1} , and is marginally detectable with HST.

In the course of our computational study we were compelled to introduce a rescaling scheme in order to numerically follow the accretion history and light curve for several years. The huge dynamical range of pertinent time scales renders a full scale time-integration numerically impractical. Our solution has been to study a scaled model which evolves more quickly and allows a simple relation between the properties and history of the rescaled model and the true one. We note that this scheme, which is presented in detail in the appendix, is potentially suitable for other problems which involve time-dependent radiation hydrodynamics spanning a large dynamic range.

We begin our discussion in § 2 with a summary of the characteristic features of supernova light curve evolution when accretion onto a central black hole is occurring. Quantitative relations between the light curve magnitude and the relevant time scales are also reviewed. The principal features of the numerical code of Zampieri et al. (1998a) and the modifications incorporated for this work are described in § 3. The light curve of SN1997D is examined in detail in § 4, where we present analytic and numerical results, including our estimates regarding black hole emergence. Prospects of observing black hole

⁵It is noteworthy that magnetic dipole emission of a Crab-like pulsar would deposit energy in the envelope at a similar rate (Woosley et al., 1989).

emergence in other supernovae are discussed in § 5, and further discussion and conclusions are offered in § 6.

2. THE SUPERNOVA LIGHT CURVE INCLUDING ACCRETION

The bolometric luminosity that follows the explosion of a massive star is powered by the internal energy of the expanding envelope, emitted as thermal photons. Under “bolometric” we do not include the hard X-ray and γ -ray photons that are emitted in radioactive decays and escape from the envelope before thermalization. In most core collapse supernovae, luminosity in the early (up to tens of days) light curve is powered by energy deposited in the envelope by the supernova shock. After this energy is depleted, only ongoing sources of energy can continue to power the later part of the light curve, often referred to as a “tail”. By definition, radiative emission from late fallback qualifies as an ongoing source, as do decays of radioactive elements in the envelope⁶.

It is useful to examine the evolution of the light curve in terms of the key characteristic time scales and luminosity scales, which can be estimated on the basis of the explosion energy and the average properties of the progenitor (Arnett 1980, 1996). When accretion onto the central object caused by late-time fallback is taken into account, additional time scales and a luminosity scale must also be included (Zampieri et al., 1998a). We briefly review these basic estimates below. They will serve also as the basis for establishing the rescaling scheme presented in the appendix.

2.1. Expansion

For an envelope with initial radius R_0 and outer velocity V_0 we can define an initial *expansion time scale*, t_0 , as

$$t_0 = \frac{R_0}{V_0}. \quad (1)$$

Assuming that after the passage of the shock the envelope settles into free streaming and homologous expansion (as is typical in strong spherical shocks), the initial velocity of a shell at radius r in the expanding envelope is simply $v_0(r) = r/t_0$. For free streaming the radius of the shell will follow $r \sim t$, and since the expansion is nearly adiabatic, the temperature T and density ρ of the radiation-pressure dominated gas decline according to $T \sim t^{-1}$ and $\rho \sim t^{-3}$. These quantities determine the leakage rate of thermal photons from the envelope material, and hence govern the history of the early light curve.

2.2. Diffusion

During the time that the initial internal energy is the dominant source for radiative luminosity, the evolution of the light curve is governed by the properties of the optically-thick, hydrogen-rich outer layer, that holds most of this energy. We denote the mass, initial average density and initial average temperature of this layer as M_H , $\rho_{0,H}$ and $T_{0,H}$, respectively.

The initial post-shock temperature of the envelope is generally high enough ($T_{0,H} \gtrsim 10^6$ °K) so that the envelope material is highly ionized, and the dominant source of opacity, κ , is Thomson scattering. Correspondingly, the thermal photons are mostly trapped in the envelope, and a radiative luminosity occurs through diffusion of thermal energy to the surface. For

a homogeneous expanding envelope this diffusion luminosity can be approximated by (Arnett, 1996)

$$L_{diff}(t) = L_{diff,0} e^{-(t_0+t^2/2)/(t_0 t_{diff,0})}, \quad (2)$$

where

$$L_{diff,0} = \frac{(\frac{4}{3}\pi\beta ac)T_{0,H}^4 R_0^4}{\kappa M_H}, \quad t_{diff,0} = \frac{3\kappa\rho_0 R_0^2}{\beta c}, \quad (3)$$

with β a numerical factor which depends on the temperature profile. The value $\beta = 13.8$ (exact for the “radiative-zero” temperature profile, $T_0(r) = T_0(\sin(\pi\frac{r}{R_0})/(\pi\frac{r}{R_0}))^{1/4}$) is usually a reasonable estimate (Arnett, 1980). The time dependence of equation (2) includes the expansion time t_0 and the initial diffusion time $t_{diff,0}$, which is the characteristic time scale for radiation to cross the envelope through diffusion at the onset of expansion. The characteristic time for radiation to diffuse out of the *expanding* envelope is given by (Zampieri et al., 1998a)

$$\begin{aligned} t_{diff} &\approx \sqrt{t_0 t_{diff,0}} = \left[\frac{1}{4\pi} \kappa M_H \right]^{1/2} \frac{1}{(cV_0)^{1/2}} \\ &\equiv \left[\frac{1}{3} \kappa R_0^3 \rho_{0,H} \right]^{1/2} \frac{1}{(cV_0)^{1/2}}. \end{aligned} \quad (4)$$

The diffusion approximation breaks down when expansion makes the envelope transparent to its thermal photons, after a typical time

$$t_{trans} \approx \left[\frac{3}{4\pi} \kappa M_H \right]^{1/2} \frac{1}{V_0} \equiv [\kappa R_0^3 \rho_{0,H}]^{1/2} \frac{1}{V_0}, \quad (5)$$

which is significantly longer than t_{diff} . However, the onset of recombination in the envelope usually occurs early enough so that the actual value of t_{trans} is irrelevant.

2.3. Recombination

As the temperature of the envelope is gradually degraded by expansion, it eventually reaches the characteristic recombination temperature of the envelope material. In a hydrogen-rich envelope this temperature can be estimated by $T_{rec,H}$ (approximately 10^4 °K), so that for adiabatic expansion we find a *recombination time scale*

$$t_{rec} = t_0 \frac{T_{0,H}}{T_{rec,H}}. \quad (6)$$

The main impact of recombination in the context of the light curve is that it imposes a sharp decrease in the opacity to the envelope’s own thermal photons: as the envelope material recombines, it rapidly transforms from opaque to transparent. This process is rapid enough so that the photons cannot readjust to the global thermal profile of the envelope; rather, a recombination “front” sweeps inward through the envelope (but outward in the laboratory frame), essentially liberating all the thermal energy which is still stored in the envelope at the time t_{rec} . As the envelope material recombines, it rapidly transforms from opaque to transparent. In many Type II supernovae the time until adiabatic expansion cools the envelope to the recombination temperature is usually smaller or equal to the diffusion

⁶Young & Branch (1989) pointed out that if the energy generation from radioactive decays is sufficiently high and the progenitor radius is sufficiently small, radioactive decays can become the dominant source of power for the light curve even very early after the explosion. They suggest that this is the case in Type II-linear supernovae.

time scale and significantly shorter than the transparency time scale, so a significant fraction of the initial thermal energy is still available at the time of recombination. This energy is then released over the time required for the hydrogen envelope to recombine, generating what is usually an observable peak in the light curve (SN1987A providing a proto-typical example). Roughly, the average luminosity during the recombination peak can be estimated as

$$\bar{L}_{rec} = \frac{E_{thermal}(t_{rec})}{t_{rec}} = \frac{4\pi R_0^3 a T_{0,H}^2 T_{rec,H}^2}{3 t_0}, \quad (7)$$

assuming that energy losses due to photon diffusion have been negligible, which is a good approximation if $t_{rec,H} < t_{diff}$. In equation (7) a is the radiation constant. Note that the nonlinear nature of the physics governing the propagation of the recombination front through the envelope limits the applicability of using the average quantities of the envelope to fully describe the light curve during the recombination phase (see more detailed estimates in Nomoto et al. 1994, Arnett 1996).

2.4. Radioactive Heating

A complete analysis of a realistic light curve must also include the effects of heating due to decays of radioactive isotopes synthesized in the explosion. After recombination, we can estimate that the envelope is practically transparent to its thermal photons, so that the luminosity due to radioactive heating is roughly equal to the instantaneous energy deposition rate due to the decays, through thermalization of the decay products. The rate of energy deposition in the envelope by the decays of an initial total mass M_X of a given isotope X can be expressed as:

$$Q_X(t) = M_X (\varepsilon_{X,\gamma} f_X(t) + \varepsilon_{X,e^+}) e^{-t/\tau_X}, \quad (8)$$

where τ_X is the life-time of the element X . The form of equation (8) distinguishes between the photons (γ -rays) and positrons emitted in the decays (with energy rates per unit mass of $\varepsilon_{X,\gamma}$ and ε_{X,e^+} respectively) since γ -rays are not totally trapped in the envelope, and their contribution to heating is modified by a trapping factor, $f(t)$. On average, the hard photons lose about half their energy in every scattering, until their energy is degraded to tens of keV. At these energies free-bound absorption on heavy elements becomes the dominant source of opacity and the photons are thermalized rapidly. Because the γ -ray opacity rises very rapidly with decreasing energy, we can assume to first order that once a hard photon scatters it is absorbed. The trapping factor can be simply approximated as (Woosley et al., 1989)

$$f_X(t) = 1 - \exp\left(-\kappa_{\gamma,X} \Phi_0 \left(\frac{t_0}{t}\right)^2\right), \quad (9)$$

where $\Phi_0(t/t_0)^2$ and $\kappa_{\gamma,X}$ are the γ -ray column depth and opacity for the typical photons emitted in the decays of element X . Since the inner (more dense) layers are the dominant contributors to the optical depth for γ -rays, the helium-rich layer can be used to estimate the total γ -ray optical depth. The time-dependent column depth is

$$\begin{aligned} \Phi_0 \left(\frac{t_0}{t}\right)^2 &\approx \int \rho dr \approx \rho_{He}(t) R_{He}(t) = \rho_{He,0} \left(\frac{t}{t_0}\right)^{-3} V_{He,0} t(10) \\ &= \left(\frac{3M_{He}}{4\pi}\right)^{1/3} \rho_{He,0}^{2/3} \left(\frac{t_0}{t}\right)^2. \end{aligned}$$

In equations (9-10) it is implicitly assumed that the expansion time t_0 is universal to the entire envelope; otherwise, it must be replaced with the characteristic expansion time of the helium-rich layer. Note that equation (10) allows us to express the trapping factor in terms of the initial (and presumably known) global quantities of the helium-rich layer. The quantity $\rho_{0,He} t_0^3$ (which appears here to the power $\frac{2}{3}$) is a useful one also in the context of accretion (see Chevalier 1989, and in detail below).

In addition to the characteristic time τ_X , another characteristic time involving radioactive heating is the γ -transparency time, similarly to equation (5). Since γ -rays carry the bulk of the energy emitted in the radioactive decays, it is important to compare this time,

$$\begin{aligned} t_{trns-\gamma,X} &= \left[\frac{3}{4\pi} \kappa_{\gamma,X} M_{He} \right]^{1/2} \frac{1}{V_{0,He}} \quad (11) \\ &\equiv [\kappa_{\gamma,X} R_{0,He}^3 \rho_{0,He}]^{1/2} \frac{1}{V_{0,He}}, \end{aligned}$$

with the other characteristic times governing the light curve history. At times $t \gtrsim t_{trns-\gamma,X}$ some of the hard photons emitted in the decays of element X escape before thermalizing and do not contribute to the bolometric light curve. We note again, that equation (11) assumes, as before, that the bulk of the envelope's opacity to hard photons is contributed by the helium-rich layer. The relevant radioactive isotopes for powering the light curve are ^{56}Ni and its daughter nucleus ^{56}Co , ^{57}Co and ^{44}Ti . We adopt the characteristic parameters for these isotopes from Woosley et al. (1989), listed in table 2.4. Note that in a realistic application, especially when the early history of the envelope is of interest, the ^{56}Co mass must be adjusted according to its production rate in ^{56}Ni decays (Shigeyama & Nomoto, 1990),

$$M_{^{56}\text{Co}}(t) = M_{^{56}\text{Ni}}(t=0) \left[\exp(-t/\tau_{^{56}\text{Co}}) - \exp(-t/\tau_{^{56}\text{Ni}}) \right]. \quad (12)$$

TABLE 1

The relevant radioactive isotopes for powering a supernova light curve: Energy emission rates in γ -rays and positrons, life-times and effective γ -ray opacities at the characteristic photon energies ^a

isotope	ε_{γ} (ergs s ⁻¹)	ε_{e^+} (ergs s ⁻¹)	τ (days)	κ_{γ}/Y_e^T ^b (cm ² /gm)
^{56}Ni	3.90×10^{10}	0	8.8	0.06
^{56}Co	6.40×10^9	2.24×10^8	111.3	0.06
^{57}Co	6.81×10^8	0	391.0	0.144
^{44}Ti	2.06×10^8	6.536×10^7	3.28×10^4	0.073

^aadapted from Woosley et al. 1989.

^b Y_e^T = the total fraction (bound and free) of electrons per nucleon

2.5. Accretion

Late-time fallback onto the black hole can be characterized in terms of the ratio of the initial expansion time scale t_0 and the initial accretion time scale,

$$t_{acc,0} = \frac{GM_{BH}}{c_{s,0}^3(\text{He})}, \quad (13)$$

where M_{BH} is the black hole mass and $c_{s,0}(\text{He})$ is the initial sound speed in the helium rich layer, which we assume is the source of material for late-time accretion. The hierarchy of these two time scales determines the hydrodynamic evolution

of the accretion flow (Colpi et al., 1996). If $\tilde{k} \equiv t_{acc,0}/t_0 \gg 1$, the gas has no time to respond to pressure forces, and accretion proceeds in a dust-like (pressure-free) manner from its onset. Alternatively, if $\tilde{k} \ll 1$ initially, accretion is at first almost unaffected by expansion and follows a sequence of Bondi-like (Bondi 1952) quasistationary states with a slowly decreasing density at large distance. Even in this latter case the flow does eventually become dust-like, since expansion continuously decreases the density and pressure in the reservoir of bound material. The transition is expected when the actual expansion and accretion time scales become comparable, yielding a *transition time* (Colpi et al., 1996)

$$\frac{t_{tr}}{t_{acc,0}} \approx \left(\frac{9}{2}\right)^{1/(9\Gamma-11)} \tilde{k}^{-9(\Gamma-1)/(9\Gamma-11)}, \quad (14)$$

where Γ is the adiabatic index of the gas. Thus $t_{tr} \approx \frac{9}{2}\tilde{k}^{-3}t_{acc,0}$ for $\Gamma=4/3$ and $t_{tr} \approx \left(\frac{9}{2}\right)^{-1/4}\tilde{k}^{-3/2}t_{acc,0}$ for $\Gamma=5/3$.

The hierarchy of time scales reflects the corresponding hierarchy of radii, when comparing the marginally bound radius, R_{mb} with the accretion radius, R_{acc} . Initially

$$R_{mb,0} = (2GM_{BH}t_0^2)^{1/3}, \quad R_{acc,0} = \frac{GM_{BH}}{c_{s,0}^2(\text{He})}, \quad (15)$$

so that if $R_{acc,0} \ll R_{mb,0}$, the initial accretion is Bondi-like. As the envelope expands $R_{acc} \sim t$ while $R_{mb} \sim t^{2/3}$ (Colpi et al., 1996), so that, as in the case of time scales, eventually the accretion will become dust-like, even if it had begun as a fluid one. The transition time t_{tr} roughly corresponds to the time when $R_{mb} = R_{acc}$.

If $t_{acc,0}/t_0 \gg 1$, pressure forces are never dominant and the late time accretion rate from an homologously expanding envelope can be estimated by the dust-like solution of Colpi et al. (1996). They find that the ratio of the dust-accretion rate \dot{M} to the Eddington accretion rate \dot{M}_{Edd} (see below) is

$$\frac{\dot{M}}{\dot{M}_{Edd}} \simeq \frac{4\pi^{2/3}}{9} \rho_{0,He} t_0 \kappa c \left(\frac{t}{t_0}\right)^{-5/3}. \quad (16)$$

The resulting luminosity produced by late-time fallback can be computed by including radiation in the calculation. A self-consistent analysis of the *radiation*-hydrodynamic evolution of the accretion flow from an expanding envelope (Zampieri et al., 1998a) shows that, at sufficiently late times, the evolution of the flow always proceeds as a sequence of quasistationary states. This is because the dynamical time scale at the accretion or marginally bound radius is much longer than all the relevant time scales of the flow and the radiation field in the inner accreting region. Both pressure and radiation forces are negligible at late times, and the flow is indeed dust-like and accretion rate declines as $t^{-5/3}$. If initially $t_{acc,0}/t_0 \gtrsim 1$ and radiation pressure is always negligible throughout the evolution, \dot{M} is given by equation (16) with the initial characteristic parameters of the bound material. On the other hand, if $t_{acc,0}/t_0 \lesssim 1$ and the accretion begins as a fluid flow, the late time accretion will still settle on a dust-like solution with $\dot{M} \propto t^{-5/3}$, but with a modified (reduced) absolute magnitude.

As a consequence of the quasi-stationary evolution of the flow and the radiation field, the late-time luminosity produced

by fallback from the expanding envelope closely follows the steady-state, spherical hypercritical accretion formula derived by Blondin (1986),

$$\frac{L_{acc}}{L_{Edd}} \simeq 4 \times 10^{-7} \left(\frac{\mu}{0.5}\right)^{-4/3} \left(\frac{\kappa}{0.4 \text{ cm}^2 \text{ g}^{-1}}\right)^{-1/3} \times \left(\frac{M_{BH}}{M_\odot}\right)^{-1/3} \left(\frac{\dot{M}}{\dot{M}_{Edd}}\right)^{5/6}, \quad (17)$$

for a given accretion rate \dot{M} . In equation (17) κ is the opacity and μ is the mean molecular weight per electron of the accreting material. The luminosity and accretion rate in equation (17) are measured in units of the appropriate Eddington quantities: the Eddington luminosity, $L_{Edd} = 4\pi GM_{BH}/\kappa = 1.3 \times 10^{38} (\kappa/0.4 \text{ cm}^2 \text{ g}^{-1})^{-1} (M_{BH}/M_\odot)$ ergs s^{-1} , and the Eddington accretion rate, $\dot{M}_{Edd} = L_{Edd}/c^2$. The evolution of the late time accretion luminosity for a dust-like flow can then be expressed as (Zampieri et al., 1998b)

$$L_{acc}(t) = L_{acc,0} \left(\frac{t}{t_0}\right)^{-25/18}, \quad (18)$$

where

$$L_{acc,0} = \Lambda \left(\frac{\mu}{0.5}\right)^{-4/3} \left(\frac{\kappa}{0.4}\right)^{-1/2} \left(\frac{M_{BH}}{M_\odot}\right)^{2/3} \rho_{0,He}^{5/6} t_{0,He}^{20/9}, \quad (19)$$

and $\Lambda \approx 1.27 \times 10^{40}$ ergs s^{-1} (for $\rho_{0,He}$ in gm cm^{-3} and t_0 in seconds) arises from the radiative efficiency of equation (17). *It is this power-law decay rate in the bolometric luminosity which characterizes the presence of a black hole in the aftermath of a supernova explosion.*

It is important to notice that equations (18) and (19) cannot apply at arbitrarily early times even if the initial conditions satisfy $t_{acc,0} \gtrsim t_0$. First, some build up time is naturally required for the accretion rate to reach a maximum and start decaying. This time should be comparable to the shorter of the two time scales t_0 and $t_{acc,0}$ ⁷. Furthermore, if during the early evolutionary stages the accretion rate can be so large that the accretion luminosity approaches the Eddington limit, radiation pressure will modify the flow even if pressure forces were initially negligible. On the basis of equation (18), we can define a critical time t_{crit} when the luminosity due to dust-like accretion equals the Eddington limit

$$t_{crit} \simeq 14.5 \left(\frac{\mu}{0.5}\right)^{-24/25} \left(\frac{\kappa}{0.4}\right)^{9/25} \left(\frac{M_{BH}}{M_\odot}\right)^{-6/25} \times \left(\frac{\rho_{0,He}}{10^{-4} \text{ gm cm}^{-3}}\right)^{3/5} \left(\frac{t_{0,He}}{1 \text{ hr}}\right)^{8/5} \text{ hrs.} \quad (20)$$

According to equation (17), the critical rate at which $L_{acc} \sim L_{Edd}$ is $\dot{M}_{crit} \gtrsim 1M_\odot \text{ yr}^{-1}$ for black holes of several solar masses. If the luminosity reaches the Eddington limit, radiation pressure cannot be ignored in comparison to the gravitational pull of the central object, and so material near the marginally bound radius (where a significant fraction of the initially bound mass resides) may receive a sufficient impulse to become unbound. Hence, we expect that if the build-up

⁷In the case of a pure dust, the build-up time can be estimated by comparing the early time accretion rate, which builds up as $\dot{M} \propto t$, (Colpi et al. 1996 (eq. [26])) to the late-time one. We find that the two become comparable at a time of $\sim 1.2t_0$.

time of the flow satisfies $\min(t_0, t_{acc,0}) \ll t_{crit}$, radiation forces will modify the accretion history and limit the accretion rate so that $\dot{M}(t \gtrsim t_{crit}) \approx \dot{M}_{crit}$ by effectively readjusting the values of $\rho_{0,He}$ and t_0 in the bound region. The total amount of bound material must be reduced as well. If, on the other hand, $\min(t_0, t_{acc,0}) \gg t_{crit}$ we can expect that radiation pressure will be of lesser significance throughout the accretion history and that, at late times, the accretion rate will settle on the dust solution of equation (16) with the original values of $\rho_{0,He}$ and t_0 (if $t_{a,0}/t_0 \gtrsim 1$).

2.6. Black Hole Emergence

We define the black hole ‘‘emergence time’’, t_{BH} , in a supernova light curve to be the time when the accretion luminosity is comparable to all the other sources of luminosity combined, i.e., $L_{acc}(t_{BH}) = \frac{1}{2}L_{tot}(t_{BH})$.

Even a small abundance of radioactive isotopes is sufficient to impose a bolometric luminosity that will initially dominate accretion luminosity, since the latter is inherently limited by the Eddington rate. However, continuous spherical accretion must eventually result in emergence, since the accretion luminosity (eq. [18]) decreases as a power law, while radioactive heating decreases at least exponentially, and even more rapidly if γ -ray trapping is incomplete (eq. [8]). Quantitatively, we expect that for any specific radioactive isotope, at a time of several times its life-time, τ_X , the heating rate is declining much more rapidly than the accretion luminosity. If the order of magnitude of the accretion luminosity and initial abundance of the dominant radioactive isotope, M_X are known, the *time* of emergence of the accretion luminosity is determined mostly by the value of τ_X , with some finer tuning due to the exact values of $L_{acc}(t)$, M_X , and the time dependence of γ -ray trapping. Note that the efficiency of γ -trapping decreases with time as $e^{(-1/t^2)}$, so the dependence of the time of emergence on M_X and L_{acc} is even weaker. Correspondingly, the *luminosity* at emergence is mostly determined by $L_{acc}(\text{several } \tau_X) \propto L_{acc,0} \tau_X^{-25/18}$.

In accordance with § 2.5, it is reasonable to assume that after a time not longer than a few $\times \min(t_0, t_{acc,0})$ the accretion luminosity is modulated to $L_{acc} \lesssim L_{Edd}$. Hence, for $\min(t_0, t_{acc,0})$ of the order of a few days, it is evident that for ‘‘typical’’ core collapse supernova, like SN1987A, with an inferred $M_{56Co} \sim 0.1 M_\odot$ and assumed $M_{44Ti} \sim 10^{-4} M_\odot$ (Woosley & Weaver, 1995), the relevant isotope for emergence is ^{44}Ti , and the time scale for emergence is $t_{BH} \approx \text{several } \tau_{44Ti} \sim \text{hundreds of years}$, at which time the accretion luminosity will drop to a few $10^{32} - 10^{33} \text{ ergs s}^{-1}$. Note that since about $\frac{1}{3}$ of the decay energy of ^{44}Ti is emitted in the form of positrons, γ -ray transparency will not affect these estimates significantly. On the other hand, in a supernova where the abundance of radioactive elements is reduced by a factor of ~ 35 , as is expected in SN1997D (see below), ^{56}Co and ^{57}Co are also relevant for examining emergence. The time of emergence is reduced to hundreds of days, and the luminosity at emergence will be a few $10^{35} - 10^{36} \text{ ergs s}^{-1}$. Of course, if no radioactive elements are present, as is expected if the mass cutoff in the supernova is very far out, emergence can occur as soon as the recombination peak clears the envelope, at 50–100 days, with $L_{acc} \gtrsim 10^{37} \text{ ergs s}^{-1}$.

3. EQUATIONS AND NUMERICAL METHOD: SUMMARY AND MODIFICATIONS

In order to explore the possibility of detecting black hole emergence in realistic supernovae in detail, we perform a nu-

merical study. Time-dependent simulation of the supernova envelope including accretion requires solution of the relativistic radiation hydrodynamic equations coupled to the moment equations for radiation transport and makes use of a detailed model for the ejecta that includes radioactive decay, realistic composition and opacities. The equations of relativistic, radiation hydrodynamics for a self-gravitating matter fluid interacting with radiation and the general relativistic moment equations for the radiation field have been presented in Zampieri et al. (1998a) (to which we refer for details). These equations were solved using a semi-implicit Lagrangian finite difference scheme in which the time step is controlled by the Courant condition and the requirement that the fractional variation of the variables in one time-step be smaller than 10%.

A fundamental obstacle in tracking the evolution of envelope expansion and accretion for several years arises from the extremely wide diversity of relevant time scales in the problem. These range from the dynamical time in the accreting region (milliseconds close to the horizon) to days for the expansion time scale, to hundreds of days for the evolution of the light curve.

Since the innermost layers of the envelope have the shortest physical time scales, the computational time can be considerably reduced with a careful choice of the location of the inner boundary. During computation, we keep the inner radial boundary of the integration domain R_{in} at hundreds to thousands of Schwarzschild radii, far outside the black hole horizon, but still but always *well within* the accreting region. This measure is acceptable because the gas in the inner accreting region is in local-thermal-equilibrium (LTE) and in near free-fall, thus allowing a reliable set of boundary conditions at R_{in} (Zampieri et al., 1998a). However, during evolution the effective optical depth in the accreting region decreases because of the secular decrease in density caused by expansion. Thus, in order to ensure that the gas is always in LTE at R_{in} , the inner radial boundary must be continuously moved inward during the simulation. We note that with this treatment, the position of the inner boundary usually limits the effects of general relativity to be quite small. However, we did not alter the general-relativistic nature of the code, especially since we cannot determine a priori how far out the inner boundary can be set (in particular at late times, when it is continuously being moved inward). Furthermore, while the accretion luminosity is insensitive to placing the inner boundary away from the black hole horizon for the canonical parameters of SN1997D, in more general scenarios it may be essential to apply the exact general relativistic formalism with an inner boundary in the strong-field domain.

Even taking advantage of the increase in the physical time scales (and hence in the time step) by suitably positioning R_{in} , the computational time needed to evolve the solution up to emergence is excessive. To reach the emergence stage in a reasonable computational time, the code employs a ‘‘Multiple Time-step Procedure’’ (MTP), originally developed by Zampieri et al. (1998a). With this technique, the integration domain is divided into several sub-grids, and each is evolved on its own characteristic time step. Starting from the same initial conditions and integration domain, the simulation performed using this MTP proved to be faster by a factor of 5–8 than one where no time-step acceleration algorithm was employed. We note that the most sensitive aspect of the MTP is maintaining accurate communication between the subgrids; correspondingly, it can be used safely only when there are no sharp features crossing the envelope (i.e., after recombination).

The main focus of the preliminary investigation of Zampieri et al. (1998a) was to study the fundamental features of fallback in a supernova and, in particular, to determine the gross properties of the accretion history and luminosity. To this end, a simplified pure-hydrogen model of the envelope, generally sufficient to produce a typical early light curve of a Type-II supernova, was adopted. Here our goal is to examine black hole emergence in realistic supernovae, and so we expand the original survey of Zampieri et al. (1998a) to take into account for variable chemical composition of the expelled envelopes, namely radial dependent abundances of various elements. In particular, we must account for the presence of radioactive isotopes and the heating of the envelope by their decays.

3.1. A Variable Chemical Composition

Inclusion of a variable composition is necessary to reproduce realistic supernova light curves, as has been established in studies of SN1987A (Woosley, 1988; Shigeyama & Nomoto, 1990). For the purpose of following the radiation hydrodynamic evolution of the accretion flow onto the black hole, chemical composition and opacity in the accreting region can have important quantitative and qualitative effects. First, there is an inherent quantitative dependence in the estimate of equation (17), which suggests that a pure hydrogen envelope produces an accretion luminosity larger by a factor of a few than a helium-metal-rich one. Furthermore, it is possible that the presence of metals in sufficient quantities may impose a qualitative change in the accretion history due to increased opacity where the material is partially ionized. Additional effects may arise through the equation of state, but in the case of supersonic accretion we expect these to be negligible.

In this work we study a supernova envelope with a mixture of hydrogen, helium and oxygen, where the relative partial fractions vary along the radial profile of the envelope. Oxygen is expected to be the most abundant heavier element in the ejected envelope, and we adopt an approximation that it represents the entire metal component in the envelope's final composition (we note that over most of the density and temperature ranges of interest, an addition of iron at solar abundance would change the frequency-integrated opacities by no more than 50%). For opacity and ionization fractions, we use the TOPS opacities available at the LANL server (Magee et al., 1995), with extrapolation to low temperatures based on Alexander & Ferguson (1994). The data are stored in the form of tables, with spacing of five entries per decade in both temperature and density for a given composition. In the course of computation the Rosseland and Plank opacities and ionization fractions are calculated with linear interpolation in temperature, density and chemical composition. The gas equation of state is approximated as an ideal gas of ions and electrons.

3.2. Radioactive Heating

For the purpose of computing the contribution of radioactive decays to the light curve, a consistent treatment of radioactive heating is required to follow the trapping efficiency, f_γ , throughout the envelope. If the rate of radioactive heating is large enough it may also affect the hydrodynamic evolution of the envelope material (there exists observational evidence for such an effect by ^{56}Ni decay in the early history of SN1987A - the "Ni-bubble", Arnett et al. 1989). The role of radioactive heating may be especially important in the case of interest here, since most of the radioactive elements are likely to lie in the inner part of the envelope, which is the reservoir for

accretion. The exact distribution will depend on the extent of mixing caused in the process of the explosion (Shigeyama & Nomoto, 1990; Bethe, 1990). Significant heating at early times may accelerate some of the material which was initially bound to the black hole and unbind it, hence imposing a smaller late-time accretion rate. On the other hand, at late times, even a small amount of heating can maintain a finite ionization fraction, which in turn will impose a larger photospheric radius, hence affecting the luminosity.

In our numerical study we introduce an effective treatment of radioactive elements by including a local heating rate. We assume that the abundance of radioactive elements is proportional to the oxygen fraction (Pinto & Woosley, 1989), with the relevant radioactive isotopes listed in table 2.4. We use the approximation discussed in § 2.4 that a γ -ray photon is absorbed after its first scattering. The trapping factor of the γ -rays emitted at radius r in the envelope can then be estimated as

$$f_{X,\gamma}(r) = 1 - \exp \left\{ - \left(\int_r^{R_{out}} \kappa_{X,\gamma} \rho(r) dr \right) \right\}, \quad (21)$$

where the quantity in parenthesis is the appropriate γ -optical depth at radius r . In our simulation we impose a further approximation that all the trapped energy is absorbed locally at the point of emission. We note that this simplified treatment of radioactive decay energy deposition is satisfactory during the first evolutionary stages when the ejecta are still very optically thick to γ -rays. Later on, however, the constant opacity/single scattering assumption gives only an approximate description of the transfer of γ -rays through the envelope. In fact, as the ejecta become marginally thick, photons can be scattered or absorbed after traveling a significant distance, making non-local effects important. An accurate calculation of the energy deposition and the γ -ray luminosity would require the solution of the energy-dependent transport problem for the γ rays, which we do not attempt. Our effective approach reduces the treatment of radioactive heating to an additional local energy source. By determining the total deposited energy rate

$$Q = \sum_X Q_X, \quad (22)$$

through equations (8) and (21), we modify the energy equation (eq.[25] of Zampieri et al. 1998a) by adding the energy input from radioactive decay

$$\epsilon_t + \tilde{a} k_p (B - w_0) + p \left(\frac{1}{\rho} \right)_{,t} = Q, \quad (23)$$

where P , ρ and ϵ , are the pressure, mass density and internal energy per unit mass of the gas, \tilde{a} is related to the 00 coefficient of the spherically symmetric, comoving-frame metric, κ_p is the Plank mean opacity, $B \equiv aT^4$ and $4\pi w_0$ is the radiation energy density (see Zampieri et al. 1998a for details). All these quantities are measured in the comoving frame.

With the aid of this modified numerical code and our analytic estimates we now proceed to study the evolution and light curve of realistic supernovae including fallback onto a nascent black hole. Our emphasis in this work is the peculiar Type II SN1997D, that may provide the first direct observational evidence of black hole formation in supernovae. This source is the only current candidate where an actual observation of the light curve at emergence of the black hole may be (marginally) possible.

4. BLACK HOLE EMERGENCE IN SN1997D

SN1997D was serendipitously discovered on January 14, 1997 by deMello & Benetti (1997) during an observation of the parent galaxy NGC 1536. In their analysis of the bolometric light curve and spectra, Turatto et al. (1998) found that SN1997D was an extremely peculiar Type II supernova. Modeling of the early light curve indicates that the supernova was discovered close to maximum light (hence, presumably, at the recombination peak). Adopting a distance modulus of $\mu = 30.64$ (a distance of ~ 14 Mpc to NGC 1536), implied that the maximum absolute magnitude of SN1997D was $M_V \gtrsim -14.65$ ($L_{\max} \lesssim 10^{41}$ ergs s $^{-1}$), fainter by about 2 magnitudes than typical Type II supernovae at maximum (Patat et al., 1994): SN1997D is possibly the most sub-luminous Type II supernova ever observed.

4.1. Fundamental Estimates about the character of SN1997D

The most unique feature of SN1997D in the context of black hole emergence is the very low mass of ^{56}Co deduced from the light curve tail (beginning at ~ 30 days after the first observation). The magnitude and shape of the tail are consistent with a very low abundance of ^{56}Co , $M_{^{56}\text{Co}} \approx 2 \times 10^{-3} M_{\odot}$ (Turatto et al., 1998). This important result has been recently confirmed by Benetti et al. (2000) on the basis of a new set of photometric data which extends up to 1.5 years after the explosion.

Turatto et al. (1998) found that the light curve and spectra were best reproduced with 4×10^{50} ergs explosion of a $26 M_{\odot}$ main sequence star (see Young et al. 1998 for details). The progenitor structure prior to collapse was an $8 M_{\odot}$ helium-rich core surrounded by an $18 M_{\odot}$ hydrogen-rich envelope. The remnant formed in the supernova is expected to have a total mass of about $3 M_{\odot}$, composed of a $1.8 M_{\odot}$ collapsed core and about $1.2 M_{\odot}$ of material which was accreted in early fallback (T. R. Young 1999, private communication). The large amount of fallback is a consequence of the low explosion energy, and provides a natural explanation for the very low observed ^{56}Co mass. Since $3 M_{\odot}$ is almost certainly larger than the maximum mass of neutron stars (even a rapidly rotating one; Cook, Shapiro & Teukolsky 1994), we can expect that a black hole was formed by SN1997D.

We note that a different model of a low mass ($\sim 8 M_{\odot}$) progenitor was suggested by Chugai & Utrobin (1999) to explain the early light curve, as well as a low ^{56}Co abundance. In such an explosion little fallback would have occurred and the remnant would be most likely a neutron star. The late time light curve shows no evidence of the presence of a neutron star (Benetti et al., 2000), which would have been observable if it were a Crab-like pulsar, or if it was spherically accreting from late-time fallback. Hence a black hole (and therefore a massive progenitor) is more consistent with the existing photometric data.

Assuming that the black hole model for SN1997D is correct, its remnant includes a black hole surrounded by a low-velocity ejecta with a small abundance of radioactive elements. If late-time fallback is proceeding in spherical accretion, the black hole could emerge rather early, while it is still potentially detectable. With a preliminary analytic estimate, Zampieri et al. (1998b) found that emergence could occur as early as three years after the explosion and that the accretion luminosity at the time is roughly in the range $10^{35} - 5 \times 10^{36}$ ergs s $^{-1}$.

We have reconsidered black hole emergence in SN1997D to determine if the accretion tail persists in a realistic model of

the ejecta that includes a variable composition, realistic opacities and radioactive heating and takes into account the radiation hydrodynamic evolution of the helium mantle starting from the conditions at few tens of hours after the explosion. In the following we attempt to constrain the luminosity at the epoch of emergence, using both analytic estimates and numerical simulations.

4.2. Analytic Estimates for SN1997D

In an analytic approach, we can use the average quantities of the helium-rich layer to estimate the radioactive heating and accretion luminosities, since this layer is expected to be both the source of material for late time fallback and the main contributor to γ -ray trapping. As a reference composition of the bound material we use the best fit model of Young et al. (1998) (see below) which is – by mass – H:0.10, He:0.45, O:0.45. The electron scattering opacity at full ionization is $\kappa_{es} = 0.22$ and the atomic weight per electron is $\mu \approx 1.27$.

4.2.1. Initial Density and Expansion Time Scale

Note that for initially homologous expansion, the total kinetic energy of the layer can be related to its total mass, M , and radius, R , according to

$$E_{kin} = \frac{3}{10} M V^2 = \frac{3}{10} M \left(\frac{R}{t_0} \right)^2, \quad (24)$$

where V is the velocity at the outer radius and $t_0 \equiv R/V$ is the corresponding expansion time scale. By expressing the radius in terms of the mass and initial average density, ρ_0 we can write

$$(\rho_0 t_0^3)^2 = \left(\frac{3}{10} \right)^{3/2} \frac{3}{4\pi} M \left(\frac{M}{E_{kin}} \right)^{3/2}. \quad (25)$$

Equation (24) is especially convenient, since the average energy per unit mass deposited in a roughly homogeneous layer is relatively easily determined in simulations (see Woosley 1988 for SN1987A). The fraction of the total explosion energy carried as kinetic energy of the helium-rich layer is typically a few percent. Adopting the global quantities of the model of Turatto et al. (1998), we have in the case of SN1997D a helium-rich layer with $M_{He} \approx 5 M_{\odot}$, $E_{kin,He} \approx 1.2 \times 10^{49}$ ergs, or $E_{kin,He}/M_{He} \approx 1.2 \times 10^{15}$ ergs gm $^{-1}$. For this layer

$$\rho_0 t_0^3 \approx 9.4 \times 10^9 \text{ gm cm}^{-3} \text{ s}^3. \quad (26)$$

Note that the relatively low energy of the explosion is clearly reflected in this quantity, which for SN1987A is only $\sim 10^9$ gm cm $^{-3}$ s 3 (Chevalier, 1989).

The value of $\rho_0 t_0^3$ is sufficient for estimating γ -ray trapping (eq. [11]), but additional information is required for estimating the accretion luminosity, which scales as $(\rho_0 t_0^3)^{5/6} t_0^{-1/4}$ (eq. [18]). This difference is an inevitable consequence of the fact that the bound material is not actually expanding homologously, since the gravitational deceleration cannot be neglected. For a realistic supernova envelope there is no time instant when the entire envelope is in coherent homologous motion. As a first approximation, we assume that the entire envelope has a common expansion time, which turns out to be $t_0 \approx 30$ hrs for an initial radius of 2×10^{13} and a hydrogen envelope of $18 M_{\odot}$.

We also have $\rho_{He,0} \approx 7.45 \times 10^{-6} \text{ gm cm}^{-3}$ for these parameters. The total mass bound to a black hole of $3 M_{\odot}$ is then

$$M_{bnd} = \frac{4\pi}{3} \rho_{He,0} R_{mb,0}^3 = \frac{8\pi}{3} GM_{BH} t_0^2 \rho_{0,He} = 0.136 M_{\odot}, \quad (27)$$

where we have used equation (15).

4.2.2. Accretion Time Scale

Homologous expansion implies that the thermal energy is sufficiently smaller than the kinetic energy. In particular, in order to have $E_{th}/E_{kin} \lesssim 0.1$ for the helium-rich layer presented above, the temperature in the layer must be $T_{0,He} \lesssim 8 \times 10^5 \text{ }^{\circ}\text{K}$. The corresponding gas and radiation pressure are of similar magnitude, leading to an estimate of the initial sound speed in this layer of $c_{s,0}(\text{He}) \approx 10^7 \text{ cm s}^{-1}$. The initial accretion time is thus $t_{acc,0} \approx 120$ hours, significantly longer than the expansion time scale. In this analytic estimate, the accretion flow is approximately dust-like from its onset. As long as we assume that the total thermal energy is the order of $\sim 10\%$ of the kinetic energy of the helium layer, which itself is well constrained, the temperature in this layer is approximately fixed at the above value. The initial gas pressure scales as $P_0 \sim T\rho_0$, so the sound speed cannot decrease significantly below $c_{s,0}(\text{He}) \approx 10^7 \text{ cm s}^{-1}$ (if the pressure is gas dominated $c_{s,0}^2(\text{He}) \propto P_0/\rho_0 \propto T$), and the initial accretion time scale (13) cannot deviate sharply from $t_{acc,0} \approx 100$ hrs, even if the combination of ρ_0 and t_0 is allowed to vary.

4.2.3. Critical Time

A key feature in this analytic estimate is that $t_{crit} \approx 180$ hrs (eq. [20]) or $\sim 6t_0$. As discussed in § 2, dust-like accretion should require a time of about t_0 to settle into the late-time temporal decay. Hence it is likely that radiation forces will impose some modification to the accretion flow. We can expect that when the accretion flow finally resettles on a dust-like motion the total bound mass will be reduced, and the average density and expansion time in the bound region will be modified. The initial values of ρ_0 and t_0 can thus provide an upper limit on the late time accretion rate and luminosity through equations (16) and (18).

The effect of radiation pressure on the early-time accretion flow when the luminosity is close to the Eddington limit is non-linear, and therefore cannot be ascertained from our analytic treatment. However, by making two simplifying assumptions we can roughly estimate the impact of the Eddington-limited stage on the late-time accretion rate. First, we assume that the accretion flow adjusts so that the accretion luminosity is exactly the Eddington value. Effective gravity is then negligible everywhere. Thus, while the average density $\tilde{\rho}_0(t)$ and expansion time $\tilde{t}_0(t)$ maintain a constant $\tilde{\rho}_0(t)\tilde{t}_0(t)^3 = \rho_0 t_0^3$, individually they vary according to

$$\tilde{\rho}_0(t) = \left(\frac{R_0 + V_0 t}{R_0} \right)^{-3}, \quad \tilde{t}_0(t) = t_0 \left(\frac{R_0 + V_0 t}{R_0} \right). \quad (28)$$

The combination $\rho_0 t_0^{8/3}$, which determines the magnitude of the dust-like accretion rate (eq. [16]) evolves as

$$\tilde{\rho}_0(t)\tilde{t}_0^{8/3}(t) = \rho_0 t_0^{8/3} \left(1 + \frac{t}{t_0} \right)^{-1/3}. \quad (29)$$

The second assumption is that the transition to a dust-like flow is instantaneous, and that at the time of transition, t_{dust} , the values $\tilde{\rho}_0(t_{dust})$ and $\tilde{t}_0(t_{dust})$ exactly yield $\dot{M}(t_{dust}) = \dot{M}_{crit}$ through equation (16). From equation (28) we find that t_{dust} must then satisfy the relation:

$$41.15 \left(\frac{\mu}{0.5} \right)^{-4/3} \left(\frac{\kappa}{0.4} \right)^{1/2} \left(\frac{M_{BH}}{M_{\odot}} \right)^{-1/3} \times \left(\frac{\rho_{0,He}}{10^{-4} \text{ gm cm}^{-3}} \right)^{5/6} \left(\frac{t_{0,He}}{1 \text{ hr}} \right)^{5/6} \times \left(1 + \frac{t_{dust}}{t_0} \right)^{-5/18} \left(\frac{t_{dust}}{t_0} \right)^{-25/18} = 1. \quad (30)$$

The modification due to radiation pressure is that $t_{dust} < t_{crit}$, so that the late-time accretion luminosity is $L(t) = L_{Edd}(t/t_{dust})^{-25/18}$ instead of $L(t) = L_{Edd}(t/t_{crit})^{-25/18}$. We find that $t_{dust} \approx 129$ hrs, so the late time accretion luminosity will be reduced by a factor of ~ 0.633 compared to that predicted by equation (18) for the initial parameters.

Note that in the limit $t_{dust} \gg t_0$ equation (30) reduces to the form $t_{dust}^2 \propto \rho_0 t_0^3$, so t_{dust} is dependent only on the initial specific energy of the bound material. This is a natural consequence of the approximation used here, since ongoing homologous expansion eventually loses memory of the initial size R_0 (which determines t_0 and ρ_0 separately). For the values presented above, t_{dust} is larger than t_0 by only a factor of a few so the above argument is not exact, but if t_0 is confined to a reasonably small range, the late-time accretion luminosity can still be very well constrained by the specific energy of the helium-rich layer. Indeed, we find that t_{dust} varies by less than 10% when t_0 is varied in the range 20–40 hrs if $\rho_{0,He} t_0^3$ is kept fixed.

4.2.4. Radioactive Heating and an Estimate of Emergence

With all the necessary values for estimating the late-time accretion rate and γ -ray opacities, we now proceed to examine the competition between the accretion and radioactive luminosities. The exact time and luminosity at emergence depend on the abundances of ^{57}Co and ^{44}Ti in the envelope. These two isotopes are mostly produced in deeper layers than those where ^{56}Co is synthesized (especially ^{44}Ti , which is produced through Nuclear-Statistical-Equilibrium (NSE) in the innermost layers of the shocked envelope material, Timmes et al. 1996). We examine their effects with two extreme assumptions – either that they are completely absent, or that their abundances scale with that of ^{56}Co . In the latter case, using $M_{^{57}\text{Co}}/M_{^{56}\text{Co}}$ (SN1987A) = 0.0243, $M_{^{44}\text{Ti}}/M_{^{56}\text{Co}}$ (SN1987A) = 1.33×10^{-3} we obtain $M_{^{57}\text{Co}}$ (SN1997D) $\lesssim 5 \times 10^{-5} M_{\odot}$, $M_{^{44}\text{Ti}}$ (SN1997D) $\lesssim 2.7 \times 10^{-6} M_{\odot}$. Assuming that the opacity to γ -rays is independent of the accretion history (as is reasonable, since the initially bound region is a small fraction of the total helium-rich layer), we can treat the radioactive heating history as fixed once the initial combination $\rho_{0,He} t_0^3$ is given (eq. [10]).

The resulting luminosities due to accretion and radioactive heating for our reference parameters of $t_0 = 30$ hrs and $\rho_{0,He} = 7.45 \times 10^{-6} \text{ gm cm}^{-3}$ are shown in Fig. 1. If the abundances of ^{57}Co and ^{44}Ti are negligible, the total luminosity due to radioactive heating is equal to the heating rate through decays of ^{56}Co . In this case, the accretion luminosity does emerge

TABLE 1
ESTIMATES OF BLACK HOLE EMERGENCE IN SN1997D BASED ON THE ANALYTIC MODEL (SEE TEXT).

$E_{\text{He}}/E_{\text{tot}}$	$\rho_0 t_0^3$ ($10^9 \text{ gm cm}^{-3} \text{ s}$)	t_0 (hrs)	ρ_0 ($10^{-5} \text{ gm cm}^{-3}$)	t_{crit} (hrs)	t_{dust} (hrs)	t_{BH}^{a} (days)	$L_{\text{tot}}(t_{\text{BH}})^{\text{a}}$ ($10^{36} \text{ ergs s}^{-1}$)	t_{BH}^{b} (days)	$L_{\text{tot}}(t_{\text{BH}})^{\text{b}}$ ($10^{36} \text{ ergs s}^{-1}$)
0.01	48.75	20	13.11	~ 524	~ 302	1148	2.69	1090	2.91
0.01	48.75	30	3.87	~ 483	~ 301	1149	2.68	1092	2.88
0.01	48.75	40	1.63	~ 456	~ 299	1151	2.65	1095	2.85
0.03	9.38	20	2.51	~ 195	~ 131	1455	0.61	1218	0.78
0.03	9.38	30	0.75	~ 180	~ 129	1466	0.59	1216	0.72
0.03	9.38	40	0.31	~ 170	~ 128	1472	0.58	1220	0.75
0.05	4.36	20	1.17	~ 123	~ 88	$\sim 1500^\dagger$	$\sim 0.40^\dagger$	1254	0.43
0.05	4.36	30	0.35	~ 114	~ 87	$\sim 1500^\dagger$	$\sim 0.39^\dagger$	1256	0.42
0.05	4.36	40	0.15	~ 107	~ 86	$\sim 1500^\dagger$	$\sim 0.38^\dagger$	1260	0.41

^a ^{57}Co and ^{44}Ti abundances scaled according to SN1987A

^b No ^{57}Co and ^{44}Ti (only ^{56}Co)

[†] In this model the accretion luminosity does not reach 50% of the total luminosity (although it does constitute more than 40%)

with $L_{\text{acc}}(t_{\text{BH}}) = L_{^{56}\text{Co}}(t_{\text{BH}}) \approx 3.6 \times 10^{35} \text{ ergs s}^{-1}$ at a time of $t_{\text{BH}} \approx 1216$ days (April 2000), after which the light curve will settle on a power law decline rather quickly. If ^{57}Co and ^{44}Ti are present with abundances rescaled from SN1987A their impact on the luminosity at ~ 1000 days is not negligible, and accretion luminosity must be compared to the total radioactive heating (labeled $L_{\text{tot-rad}}$ in Fig. 1). In this case emergence is delayed to $t_{\text{BH}} \approx 1466$ days (December 2000), with $L_{\text{acc}}(t_{\text{BH}}) = L_{\text{tot-rad}}(t_{\text{BH}}) \approx 2.9 \times 10^{35} \text{ ergs s}^{-1}$. Note that in this case the contribution of ^{44}Ti is about $1.4 \times 10^{35} \text{ ergs s}^{-1}$, which decreases only very slowly due to increasing γ -ray transparency. Correspondingly, the total luminosity (labeled L_{tot}) does not follow a perfect power law until ^{44}Ti heating becomes negligible, although the accretion luminosity will remain the dominant source of luminosity for several thousands of days after t_{BH} .

The results of similar calculations for the emergence of a $3 M_\odot$ black hole in SN1997D for different values of the initial parameters are presented in table 1. We vary the energy of the $5 M_\odot$ helium-rich layer as 1, 3 (the nominal case) and 5 percent of the total explosion energy of $4 \times 10^{50} \text{ ergs}$, while varying t_0 in the range 20–40 hrs. We list the derived values of t_{crit} and t_{dust} for each model and the resulting luminosity and time of emergence. Due to uncertainty regarding the abundances of ^{56}Co and ^{44}Ti , we examine the two extreme cases where their abundances scale according to SN1987A, and when they are completely absent. The case of the helium-rich layer having 5% of the total energy and with the significant abundance of ^{57}Co and ^{44}Ti marks the border-line of achieving emergence after a few years (instead of in thousands of years) as the combination of ^{57}Co and ^{44}Ti heating is slightly *larger* than the accretion luminosity (by about $\sim 20\%$) for a very long time.

Our results indicate that if a black hole was formed, it is likely to emerge about three years after the explosion. Taking into account also for the uncertainties in composition and black hole mass, we estimate that plausible values of the luminosity at emergence seems to lie in the range $0.3 - 3 \times 10^{36} \text{ ergs s}^{-1}$, and the expected time of emergence is $\sim 1100 - 1500$ days after

the explosion, with higher luminosities corresponding to earlier times. We emphasize that the dominant quantity that determines the value of the luminosity at emergence is the kinetic energy of the helium-rich layer, while the time of emergence and the character of the late-time light curve are also sensitive to the possible presence of ^{57}Co and ^{44}Ti in non-negligible abundances.

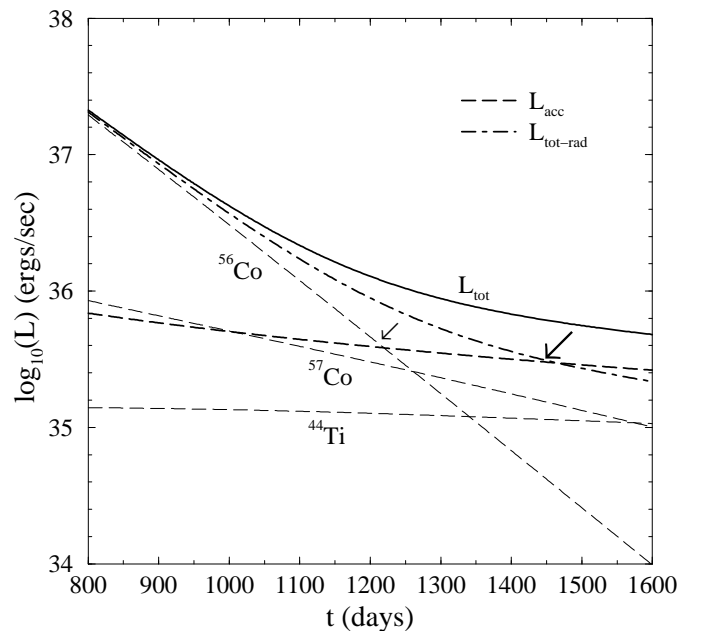


FIG. 1.— Analytic estimates for the total bolometric luminosity of SN1997D, L_{tot} , and the partial contributions of accretion onto the black hole (L_{acc}) and of radioactive heating ($L_{\text{tot-rad}} = L_{^{56}\text{Co}} + L_{^{57}\text{Co}} + L_{^{44}\text{Ti}}$) during the period 800–1600 days from the explosion (Jan. 1999–Mar. 2001). Arrows mark the time of emergence of the accretion luminosity in the case where (1) large arrow: ^{57}Co and ^{44}Ti are assumed to be present in the envelope with abundances scaled down from SN1987A (see text) and (2) small arrow: when only ^{56}Co is present.

4.3. Numerical Results for SN1997D

While an approximate analytic treatment and scaling behavior can provide useful estimates of the time and luminosity at emergence, it also underscores the need to perform numerical investigation which can track in detail the early time accretion history and the late-time evolution of the light curve. The numerical simulation is also required to quantitatively assess the role of non-linear radiation-hydrodynamics processes and the effects of variable chemical composition, realistic opacities and radioactive heating. In order to explore in detail the emergence of a black hole in SN1997D, a full radiation-hydrodynamic simulation of fallback of material from the supernova envelope up to the several years after the explosion has been performed, using the numerical code described in § 3. The initial conditions for the ejecta were based on the best-fitted model of Young et al. (1998) for the SN1997D explosion. This model of a $26 M_{\odot}$ progenitor was fitted on the base of the early time light curve (up to ~ 100 days after the explosion), which is practically independent of the inner part of the helium-rich layer. Hence, while a simulation based on this model serves as an essential quantitative estimate, the unavoidable uncertainties regarding the initial velocity, density and temperature profiles of this inner layer obviously limit the applicability of the simulation as a “best fit” also for the accretion history and luminosity.

4.3.1. Initial Profile

The initial profile describes the supernova envelope at the time of break-out of the shock at the surface, corresponding to about 13 hours after core bounce. The expanding envelope is composed of two main components: an inner helium-rich layer and an outer hydrogen-rich envelope. The properties of the profile are presented in Figs. 2 and 3 and the region of initially bound material is shown in more detail in Fig. 4. By assuming that the abundance of radioactive isotopes scales with the oxygen mass fraction, we can simply estimate the mass fraction of ^{56}Ni in every mass shell by requiring that the total ^{56}Ni mass is $2 \times 10^{-3} M_{\odot}$ (equal to the total ^{56}Co mass inferred by observations). In the simulation we assume that the abundances of ^{57}Co and ^{44}Ti scale with the abundance of ^{56}Ni , so their total masses are set according to the aforementioned quantities.

In the context of late-time accretion, the most dominant feature of the initial profile is the non-uniformity of the helium-rich layer. A significant fraction of the mass is concentrated in an over-dense region bordering with the hydrogen-rich layer. This region also holds the bulk of the kinetic energy of the helium-rich layer, 1.7×10^{15} ergs gm^{-1} , somewhat larger than the average value of 1.2×10^{15} ergs gm^{-1} mentioned above. The bound region on the other hand, is relatively under-dense and slow. The total initially bound mass is $\sim 0.22 M_{\odot}$.

The expansion time scale throughout most of the initially bound material is $t_0 \approx 50 - 60$ hrs. This region is radiation-pressure dominated, and the initial sound speed is roughly $c_{s,0}(\text{He}) \approx 1.3 \times 10^7$ cm s^{-1} . The corresponding accretion time scale, $t_{acc,0} \approx 50$ hrs is therefore similar to the initial expansion time scale. Unlike the analytic cases discussed above, in this model pressure forces are initially important. The long initial expansion time scale more than compensates for the decreased density in terms of determining the accretion rate, and we have $t_{crit} \approx 300$ hrs. This model is also expected to reach very high accretion rates at early times, which will result in some moderation of the accretion flow when $\dot{M}_{crit} \approx 3.13 M_{\odot} \text{yr}^{-1}$ is approached.

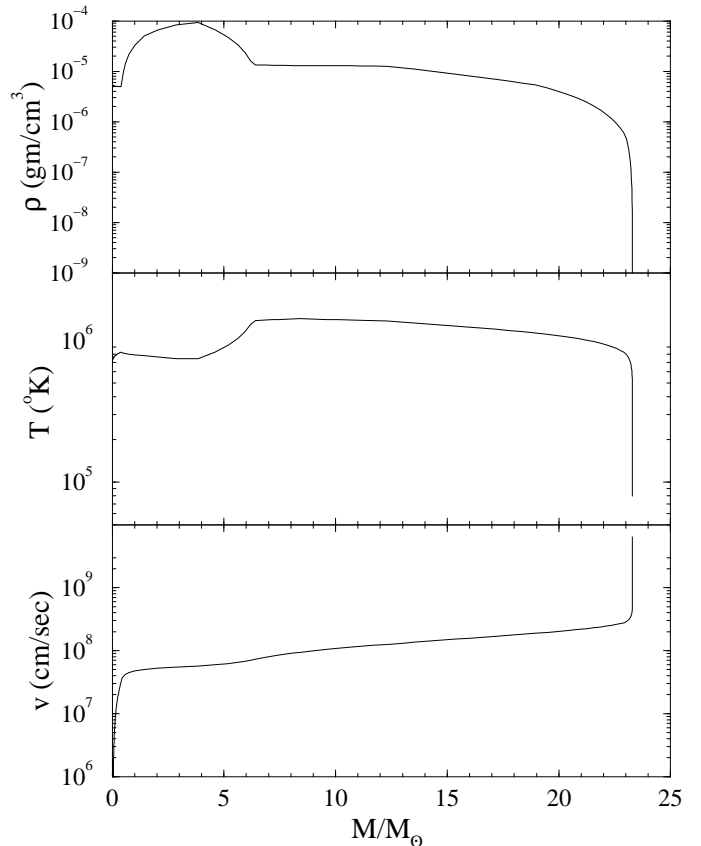


FIG. 2.— Initial SN1997D profile for the fiducial model of Young et al. (1998): the density, temperature and velocity profiles of the envelope at shock emergence (~ 13 hrs after core bounce).

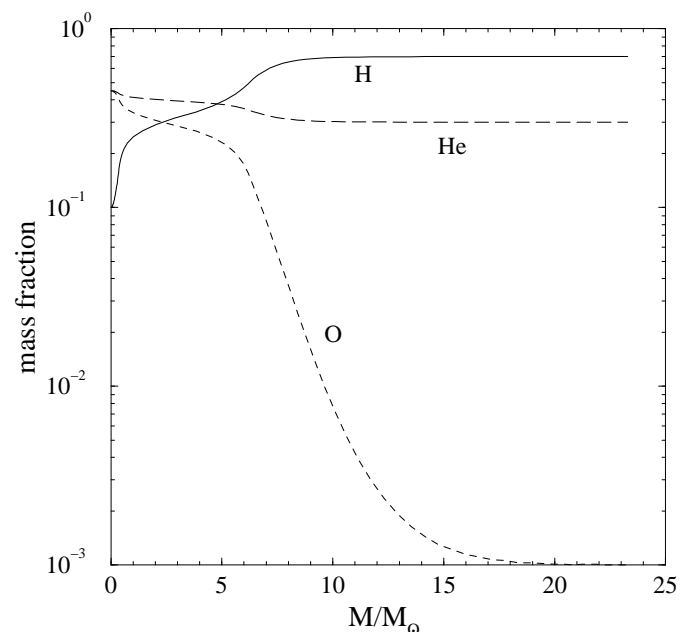


FIG. 3.— Initial SN1997D profile for the fiducial model of Young et al. (1998): the composition profile (mass fractions of H-He-O) for the envelope.

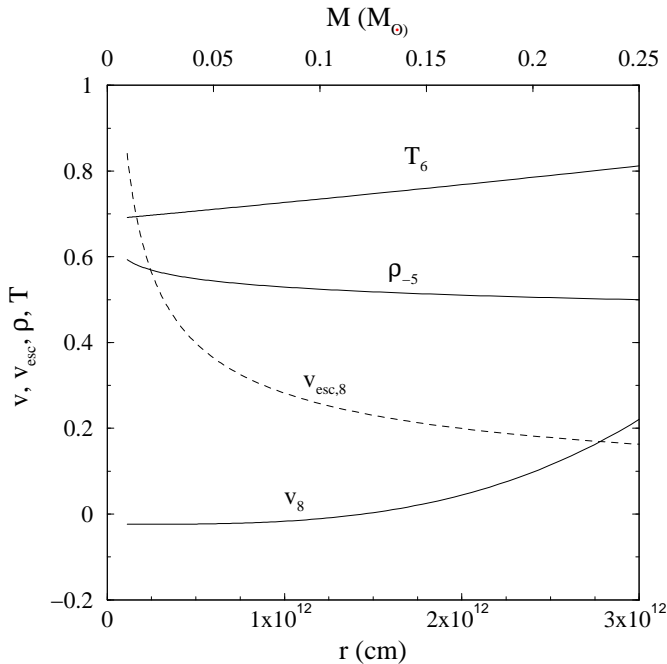


FIG. 4.— Blow up of the initial SN1997D profile of the initially bound material for the fiducial model of Young et al. (1998) at shock emergence. Plots are temperature (in units of 10^6 °K), density (in units of 10^{-5} gm cm $^{-3}$) and velocity and escape velocity (in units of 10^8 cm s $^{-1}$).

4.3.2. Computational Aspects

Tracking the evolution of the envelope over several years (the expected time of emergence of the black hole) is not feasible numerically. Integrating the model until emergence would require a CPU time greater than one month, even when adjusting the position of the inner boundary and using the MTP procedure (see § 3). As a result, we devised a rescaling scheme where the original model is rescaled to a more rapidly evolving one, while maintaining simple relations between the quantities computed for the rescaled model and the original one. This rescaling scheme, presented in detail in the appendix, has allowed for an additional acceleration of a factor of ~ 5 in computational efficiency, thus reducing the total required computational time to an acceptable limit.

We must note that several particulars of the initial model used here for SN1997D imposed some specific complications in employing the rescaling scheme. The fact that initially $t_{\text{acc}} \lesssim t_0$ and that the flow is expected to be moderated at early times when a critical accretion rate is approached implies that the rescaling scheme described in the appendix cannot be applied at the earliest stages of evolution. Furthermore, at early times the energy generation rate of the radioactive elements, and especially ^{56}Ni , is at its largest. The enhancement required for these rates in the course of rescaling (see in the appendix) further compounds the applicability of the rescaling scheme at very early times.

Therefore our numerical approach has been to perform the simulation of the model in its original scale until three conditions are met: 1) the time dependent marginally bound radius is significantly smaller (a factor of 5) than the accretion radius; 2) the accretion rate through the inner boundary is smaller than $0.1\dot{M}_{\text{crit}}$ and 3) that total energy to be emitted in the decays of the remaining ^{56}Ni is significantly smaller than the internal energy at that time. We find that these conditions are all satisfied at the physical time of about $t=25$ days, which is when the sim-

ulation was stopped, rescaled by a factor of 5, and restarted. We performed the simulation of the rescaled model with a single time-step integration until the recombination front has settled to a roughly constant Lagrangian position, which occurs after about $t = 150$ days. These first two stages required about 20 CPU hours each. From this point on, the simulation is continued with the Multi Time-step Procedure, where the integration domain was divided into four sub-grids. Performing the simulation up to a physical time of $t = 1500$ days required an additional 120 CPU hours (recall that at later times the time step drops as the inner boundary must be moved inward in order to maintain it in LTE – see § 3). All computations were performed on a SGI 500MHz EV6 machine with a compaq XP1000 processor.

4.3.3. Numerical Results

The calculated light curve for SN1997D is shown in Fig. 5. Also shown are the observed data extending up to ~ 440 days after the explosion (Benetti et al., 2000), with which the agreement of the simulated light curve is very good. For comparison, we also show the light curve calculated for an identical model but with the abundance of radioactive elements reduced by a factor of 300, and also the late-time light curve estimated analytically as in Fig. 1 above. In the simulation we cannot single-out the accretion luminosity directly, by we can evaluate its contribution to the total luminosity by subtracting the contributions of radioactive heating. The simulation does record the total rate of energy deposition in the envelope by the decays of each of the isotopes, $Q_X(t)$, and since we can estimate that the deposited heat is emitted as a bolometric luminosity very rapidly after thermalization, i.e., $L_X(t) \approx Q_X(t)$, we can attempt to identify the accretion luminosity as $L_{\text{acc}} = L_{\text{tot}} - (Q_{^{56}\text{Co}} + Q_{^{57}\text{Co}} + Q_{^{44}\text{Ti}})$. These calculated contributions for the model are shown in Fig. 6.

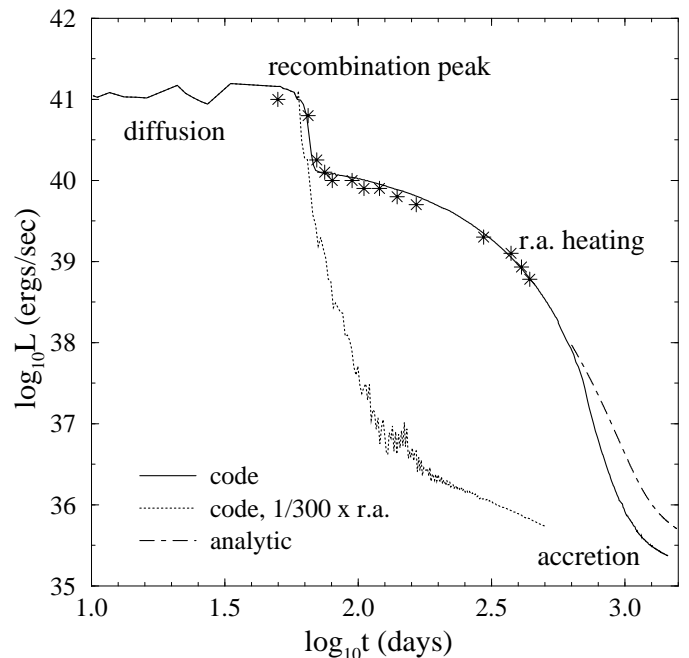


FIG. 5.— Numerical result for the bolometric light curve of SN1997D using the fiducial initial model (Young et al., 1998), and the same model with the abundance of radioactive elements reduced by a factor of 300 (solid and dashed lines respectively). Also shown are the data of observed bolometric luminosity for $t \leq 450$ days (asterisks) from Benetti et al. (2000), and the analytic estimate of § 4.2 (dot-dashed curve)

The transition from a ^{56}Co -dominated tail in the luminosity is evident at about 1000 days. From Fig. 6 we can determine that the accretion luminosity does become the dominant source of the light curve, and the time of emergence (when $L_{\text{acc}}(t_{\text{BH}}) = \frac{1}{2}L_{\text{tot}}(t_{\text{BH}})$) is $t_{\text{BH}} \approx 1050$ days, when $L_{\text{acc}} \approx 3.2 \times 10^{35}$. This is roughly $\frac{1}{5}$ of the accretion luminosity (at the same physical time) estimated using the initial average values of $\rho_{0,\text{He}} = 5 \times 10^{-6} \text{ gm cm}^{-3}$ and $t_0 = 50$ hrs in equation (18). This difference is the result of moderation by radiation forces as the accretion rate exceeds \dot{M}_{crit} , and in part also by the fact that initially the envelope's own pressure is not negligible. An accretion rate of $\dot{M} > \dot{M}_{\text{crit}}$ is actually reached while the accretion flow is still building, and the radiation pressure it induces causes a *significant part* of the initially bound material to become unbound. Indeed, the total accreted mass (extrapolated to $t \rightarrow \infty$) found in the simulation is decreased to only $\sim 0.067 M_{\odot}$, less than a third of the originally bound material.

The evolution of the accretion rate is plotted in Fig. 7, which shows the accretion rate (calculated near the inner boundary) as a function of time. The maximum accretion rate is reached after about 18 hrs, when its value is $\sim 1.5\dot{M}_{\text{crit}}$. At this stage the accretion flow is not quasi-stationary (see below), and significant moderation is imposed. We comment that the details of the accretion rate at these very early times are dependent on the assumed initial conditions. With initial conditions set during collapse, MacFadyen, Woosley, & Heger (1999) find that the earliest accretion reaches a maximum rate as early as a few hundred seconds after bounce. In our numerical simulation the initial conditions are set after the passage of the shock through the envelope and hence we cannot reproduce these earliest stages of the accretion history. More significant in the context of black hole emergence, however, is the character of the flow as it settles on the late-time, dust-accretion track, where there is good agreement between our results and those of MacFadyen et al. (1999).

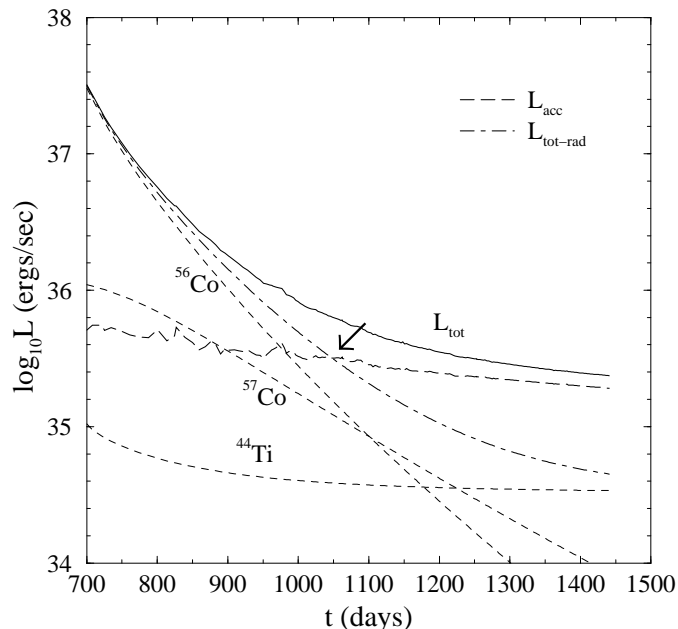


FIG. 6.— The total bolometric luminosity for the nominal model for SN1997D and the estimated partial contributions of accretion onto the black hole and of radioactive heating during over the period 700–1500 days from the explosion (Nov. 1998–Dec. 2000). The arrow marks the time of emergence of the accretion luminosity ($L_{\text{acc}} = \frac{1}{2}L_{\text{tot}}$).

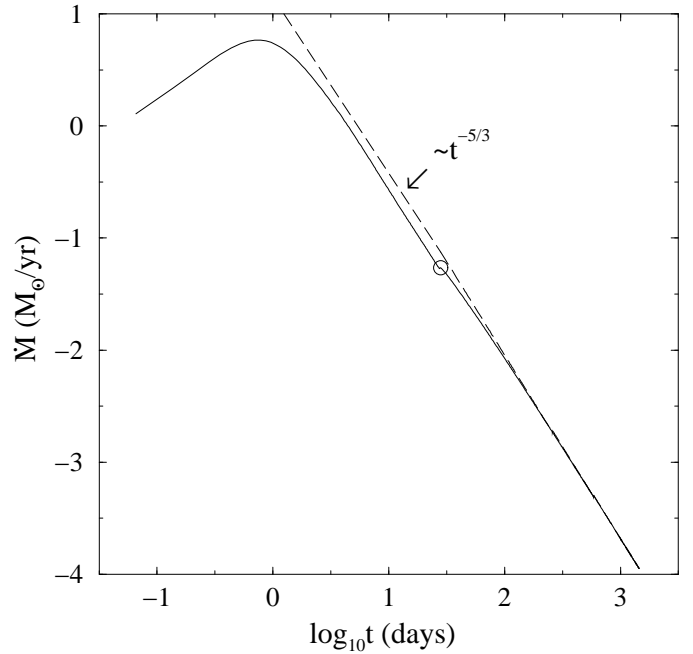


FIG. 7.— Accretion rate $\dot{M}(R_{\text{in}})$ close to the inner boundary versus time for the fiducial model. The circle denotes the transition from the original model to the rescaled one (see text).

It is apparent that the accretion does eventually settle on a dust-like flow $\dot{M} \sim t^{-5/3}$, as expected, at ~ 10 days after the explosion. The quantitative effect of the early history of the accretion flow is clearly apparent, since the accretion rate is lower than the value predicted by equation (16) for $\dot{M}(10 \text{ days})$, based on the initial properties of the inner part of the bound region. By extrapolating the dust-like accretion rate back in time, we find that $\dot{M} = \dot{M}_{\text{crit}}$ at ~ 100 hrs, instead of the original estimate of $t_{\text{crit}} \approx 300$ hrs.

We mark the time of transition between the original model and the rescaled one by a circle in Fig. 7. After a short transient, the accretion flow resettles on a dust-like accretion flow, with a very good fit (accurate to about 10%) to the initial unscaled model. This agreement suggests that the rescaled model is indeed capable of reproducing the accretion flow and luminosity.

In Fig. 8 we show the behavior of the computed accretion luminosity as a function of the computed accretion rate \dot{M} , and compare it to the analytic estimate of the Blondin formula (eq. [17]). The excellent fit of the simulation to the analytic ratio demonstrates that the radiation-hydrodynamic evolution in the accreting region does indeed follow a sequence of quasistationary states, so the analytic estimates are also justified in the case of a variable chemical composition. The reduced accretion rate is clearly the cause for the accretion luminosity being only about one fifth of its value (had the entire initially bound mass remained available for accretion).

It is noteworthy that the black hole emerges somewhat earlier than in the case of Fig. 1, in spite of the lower accretion luminosity. This is due to a significant complementary effect: the structure of the helium rich layer reduces the effective optical depth to the high energy photons emitted in the radioactive decays. First, the initial column depth of the layer is only about $\frac{1}{3}$ of that of a layer with identical mass and size but a constant density. Second, the outer part of this layer has a larger specific ki-

netic energy and therefore a smaller $\rho_0 t_0^3$ than the average value used in § 4.2. This combination causes the γ -ray column depth of the helium-rich layer to be only 1/5–1/4 of that at an identical time for an analytic estimate, and the trapping efficiency is decreased accordingly. Correspondingly, the contribution of radioactive heating to the bolometric luminosity is reduced to what would have been expected if the entire helium-rich layer were characterized with $\rho_0 = 5 \times 10^{-6} \text{ gm cm}^{-3}$ and $t_0 = 50 \text{ hrs}$.

The model with reduced radioactive isotopes was investigated in order to assess the quantitative effect of radioactive heating on the dynamics of the flow. This effects can be inferred indirectly from Fig. 5, and directly by comparing the accretion history in both models. We find that the accretion histories are practically identical, where the late-time accretion rate in the model with reduced radioactive heating is larger by only $\sim 5\%$ than in the nominal model, implying that even in the nominal model the energy deposited by heating hardly affects the region of bound material. The calculated accretion luminosities also agree to within a few percent, although it is the model with radioactive isotopes that suggests a higher luminosity. While this effect may be partially a numerical artifact, it may also arise from the slightly larger photo-spheric radius found in the original model, presumably caused by radioactive heating. We conclude that when the abundance of radioactive elements in the ejected envelope is as low as it is in the case of SN1997D, it is unlikely to impose a significant effect on the expected accretion rate or luminosity. By contrast, even the small amount of radioactive isotopes present in the SN1997D envelope is sufficient to affect the decline of the recombination peak (see Fig. 5). This effect was demonstrated clearly in the investigations of the SN1987A light curve (Woosley, 1988; Shigeyama & Nomoto, 1990), and is mainly due to release of heat deposited in the inner part of the envelope by ^{56}Ni decays.

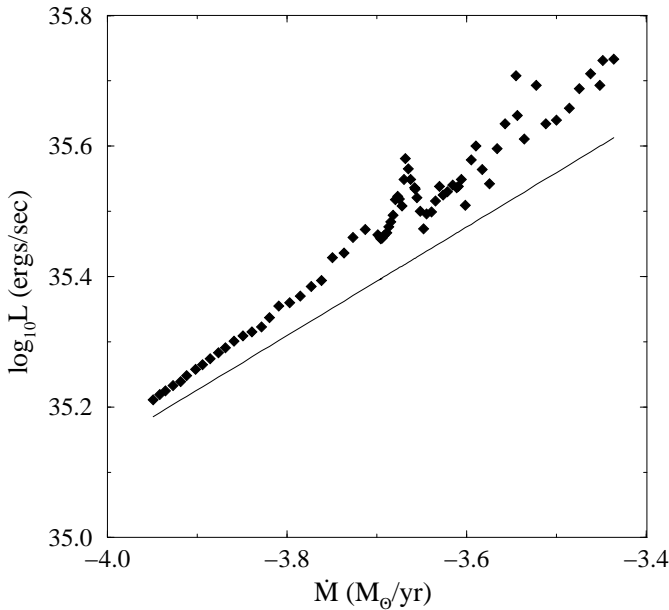


FIG. 8.— The computed accretion luminosity (Fig. 6) versus \dot{M} (diamonds) for the fiducial model of SN1997D. Also shown is the analytic estimate based on equation (17) for the chemical composition of the bound region of the helium-rich layer (mass fractions H:0.1, He:0.45, O:0.45).

The negligible effect of radioactive heating on the hydrodynamic evolution allows for a simple extrapolation regarding the expected light curve if the abundance of the relevant isotopes is

varied. If the abundances of ^{57}Co and ^{44}Ti are very low, emergence can be gauged by comparing the accretion luminosity and the heating by ^{56}Co decays, suggesting that emergence occurs at about 970 days. The luminosity at emergence would be slightly higher, with $L_{\text{acc}} \approx 3.9 \times 10^{35}$. In this case, the contribution of ^{56}Co heating declines rapidly and the late time light curve should indeed fall off as a power-law in time. Note that a perfect power law decline is found, as expected, for the model with reduced abundances of radioactive isotopes.

To conclude our investigation of the SN1997D light curve, we examine the history of the luminosity and the accretion flow throughout the envelope. The profiles of the (comoving frame) luminosity, $L(r)$, and mass flux, $|\dot{M}|(r)$, at various selected times during this evolution are plotted in Figs. 9a and 9b respectively.

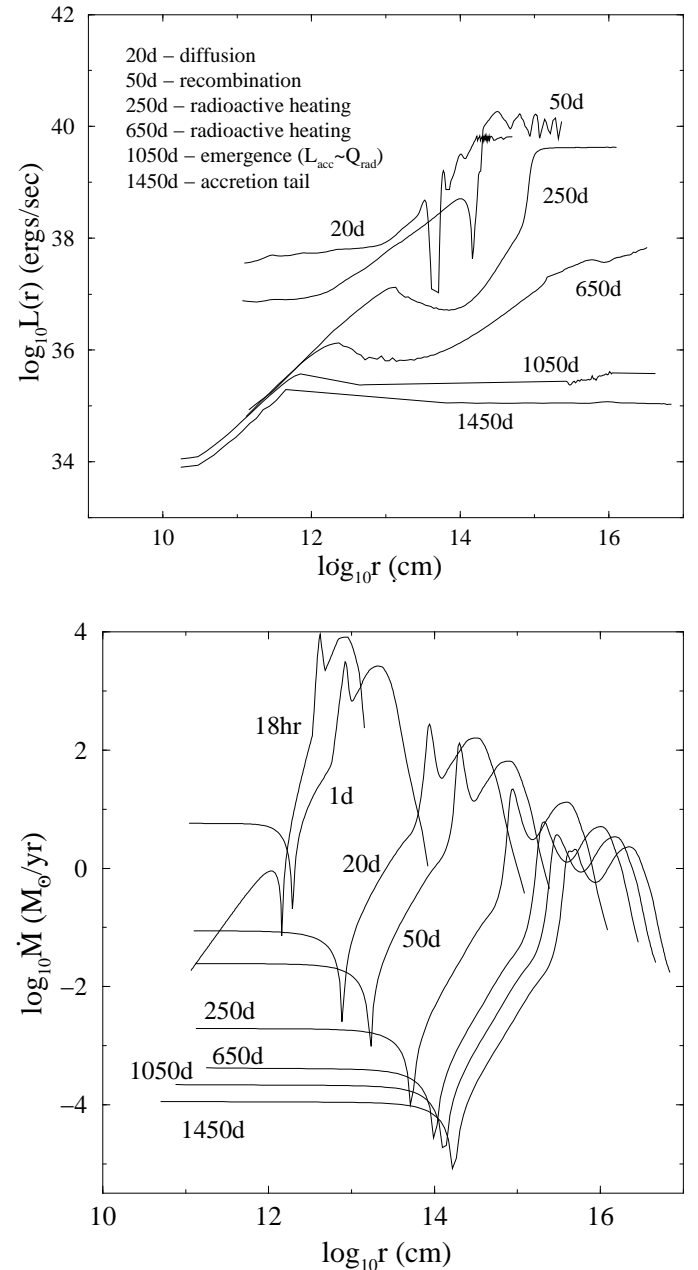


FIG. 9.— Properties of the flow at selected times for the fiducial model of Young et al. (1998) for SN1997D: (a) comoving luminosity profiles (b) mass flux profiles.

The luminosity profiles demonstrate the evolution of the light curve through its various stages (see Zampieri et al. 1998a for details). During the stage dominated by radioactive heating the photo-sphere lies well above the accreting region. The presence of a separate source of luminosity due to compressional heating in the course of accretion is evident in the inner part of the flow, but only when its magnitude becomes comparable to the heating produced by radioactive decays does it start to dominate the luminosity output. The drop in luminosity near the inner boundary arises because the opacity of the partially ionized helium-rich material becomes larger (much greater than the electron scattering opacity). Closer to the black hole the increased temperature increases the degree of ionization of the helium-rich material, and the comoving luminosity rises again to a local maxima. Note that the mass flux remains self similar through out the evolution, as the accreting region grows in size but the expansion of the envelope reduces the magnitude of the accretion rate. The sharper, inner spike in the mass flow rate is due to the original spike in density of the model at the interface between the helium-rich and hydrogen-rich layers (the smoother, outer peak simply corresponds to a maximum in the combination $\rho v r^2$). In the inner region the accretion rate is nearly independent of radius, which also reflects that the accretion flow does indeed follow a sequence of quasi-stationary states.

5. BLACK HOLE EMERGENCE IN OTHER SUPERNOVAE

While SN1997D appears to be the only existing candidate for observing black hole emergence, theory suggests that the explosions of the most massive stars in the core-collapse supernovae range would be significantly more favorable for an unequivocal determination of the presence of a black hole. The key feature is, of course, the final yield of heavy elements in the envelope following early fallback. These heavy elements include the radioactive isotopes which mask the accretion luminosity for extended times, so that the lower the abundance of radioactive elements, the shorter the time until emergence and the larger the luminosity at that time. SN1997D may be sufficiently poor in heavy elements so that the accretion luminosity can dominate the heating by ^{44}Ti decays, but ^{56}Co decays are by far the dominant source of power until ~ 1000 days after the explosion.

In a survey of the supernovae of massive stars, Woosley & Weaver (1995) concluded that explosions of stars of initial masses of $30-40 M_{\odot}$ are likely to include significant early fallback, thus advecting the newly synthesized heavy elements onto the remnant, a likely black hole. For “nominal” explosion energies of $\sim 1.2 \times 10^{51}$ ergs, they found that explosions of stars with masses of $30-40 M_{\odot}$ should easily lead to remnant masses in the range of $3-10 M_{\odot}$, while ejecting envelopes practically free of heavy radioactive elements. While they did not consider explosion energies as low as the 4×10^{50} ergs inferred for SN1997D, it is natural to assume that lower energy explosions will give rise to enhanced earlier fallback and thus higher remnant masses⁸.

In order to gauge the possible signature of black hole formation in a supernova of a very massive progenitor, we computed the light curve of such a supernova using the numerical code described in § 3. As a reference we used a $35 M_{\odot}$ progenitor

⁸Woosley & Weaver (1995) did examine explosion energies of $\gtrsim 2 \times 10^{51}$ ergs. In general, they found that if explosion energy is large enough to eject a non-negligible amount of radioactive isotopes in stars of $30-40 M_{\odot}$, the remnant mass will be $\lesssim 2.5 M_{\odot}$, and hence, possibly, a neutron star

based on model S35A of Woosley & Weaver (1995). It has a pre-explosion outer radius of 8×10^{13} cm, and is composed of a $14 M_{\odot}$ helium-rich core and a $21 M_{\odot}$ hydrogen-rich envelope. The post explosion ejecta profile was constructed so that the total ejected masses are 11.5, 12 and $4 M_{\odot}$ of hydrogen, helium and oxygen, respectively. Most notably, the envelope is assumed to be free of radioactive isotopes. The total kinetic energy of the ejecta is set at 1.2×10^{51} ergs, leaving behind a $7.5 M_{\odot}$ black hole. Assuming that the helium-rich layer carries 1% of the total energy and that the entire envelope has a common expansion time scale, our model has $t_0 \approx 55$ hrs. The initial profile of the bound material thus has $\rho_{0,He} = 4.93 \times 10^{-6}$ gm cm $^{-3}$ and therefore $\rho_0 t_0^3 = 3.83 \times 10^{10}$ gm cm $^{-3}$ s $^{-1}$. This expansion time scale is significantly shorter than the accretion time scale, which for this model is roughly 10 days, so that the flow is dust-like at its onset. The critical time is, however, ~ 280 hrs, and once again we expect the accretion can begin as dust-like and become then moderated by radiation pressure when the Eddington limit is approached. Through the analytic estimates in § 4.2 we find that $t_{dust} \approx 110$ hrs for this model.

The calculated light curve for S35A is shown in Fig. 10. We note that no rescaling was required for these models due to the relatively large time step and short evolutionary time required until emergence; the calculation required about 55 CPU hours. The modest explosion energy combined with the large radius of the progenitor lead to a relatively small initial average temperature of about 2.5×10^5 °K, and recombination occurs around a time of $t_{rec} \approx 35$ days. The light curve during this peak is quite similar to the one observed for SN1994W, a reasonable candidate for an explosion of a very massive star with very little radioactive elements in the ejecta (see below).

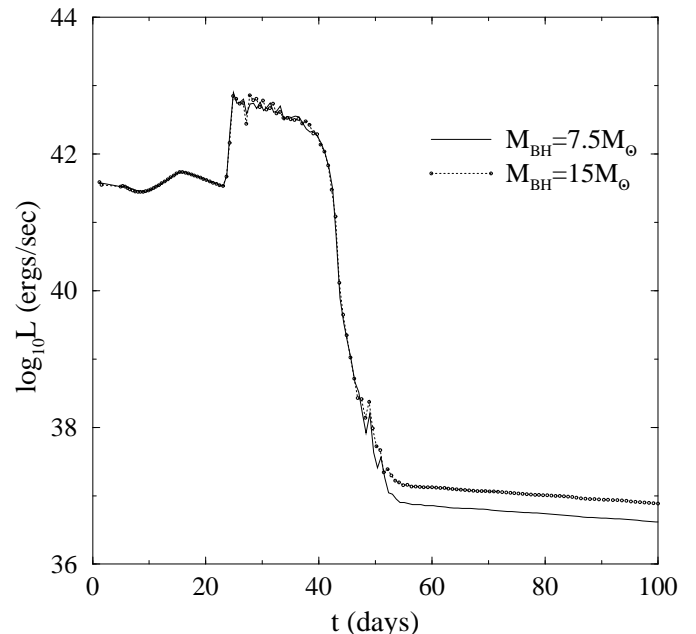


FIG. 10.— The light curve including an accretion tail for the S35A model of Woosley & Weaver (1995). Solid line: $M_{BH} = 7.5 M_{\odot}$, dashed line: $M_{BH} = 15 M_{\odot}$.

In the absence of radioactive heating the recombination peak fades rapidly, and the emergence of the black hole occurs at $t \approx 55$ days with a total luminosity at emergence of about

10^{37} ergs s^{-1} . The rapid decline of the recombination luminosity causes the accretion luminosity to be nearly the sole contributor to the light curve as early as at $t \approx 60$ days, with a luminosity of $L(t = 60 \text{ days}) \approx 7.2 \times 10^{36}$ ergs s^{-1} . This value is *smaller* than the analytic result of $L(t) = L_{Edd}(60 \text{ days}/t_{dust})^{-25/18}$ by a factor of a few, although the calculated accretion rate *does* satisfy $\dot{M}(t) \simeq \dot{M}_{crit}(t/t_{dust})^{-5/3}$. This result is due to the fact that at this stage bound-bound and bound-free opacities in the (relatively narrow) partially ionized region in the accreting material are high (much larger than free electron scattering opacity). This imposes a significant contribution to the total optical depth of the accretion flow, increasing its “effective” average opacity. Note that for a given accretion rate, the accretion luminosity is expected to follow a $L_{acc} \propto \kappa^{-1/2}$ dependence (using eq. [17] and expressing L_{Edd} and \dot{M}_{Edd} explicitly). This is a transient effect: as time elapses, expansion of the envelope gradually causes the fully ionized, inner part of the accreting region to dominate the optical depth of the flow, so that the average “effective” opacity is rapidly declining towards the electron scattering value. Consequently, at this stage the luminosity falls off somewhat more slowly than a $t^{-25/18}$ power-law, eventually settling on such a time dependence.

Also shown in Fig. 10 is the same model with the black hole mass arbitrarily increased to $M_{BH} = 15 M_{\odot}$, the light curve evolution is identical until emergence, which occurs at a slightly higher luminosity and therefore at a slightly earlier time ($\sim 3 \times 10^{37}$ ergs s^{-1} at $t \approx 50$ days). The light curve again evolves thereafter due to accretion $L(60 \text{ days}) \approx 1.33 \times 10^{37}$ ergs s^{-1} , again falling off somewhat more moderately than a $t^{-25/18}$ power law.

We emphasize that the accretion rate and luminosity in both models are significantly lower than that predicted by equations (16, 19) for the initial parameters of the helium-rich layer. Even though the accretion can begin as dust-like, the moderation of the accretion flow by radiation pressure when the Eddington limit is approached is evident in the absolute magnitude of the accretion luminosity-tail. The model with the larger black hole mass has a higher critical accretion rate, so even though it also induces a smaller t_{dust} , the ratio of the accretion luminosity is increased by slightly more than just a factor of $2^{2/3}$ arising from the ratio of the black hole masses.

We conclude, that *Type II supernovae with no radioactive isotopes provide the most favorable cases for observing the emergence of a black hole*. It is noteworthy that a similar explosion of the bare helium core in Type Ib/Ic supernovae would be far less favorable. Not only will all the explosion energy be deposited in the helium layer (instead of only a few percent), there will also be no inverse shock that slows the inner part of the helium layer and enhances fallback (which is essential for decreasing the abundance of ejected radioactive elements). The very small time step required for simulating such a model prevents us from examining it numerically, but we can place some limits with the analytic derivations presented in § 4.2. For example, consider a $14 M_{\odot}$ helium star with an initial radius of $R_0 \approx 10^{11}$ cm exploding with an energy 1.2×10^{51} ergs, producing, again, a $7.5 M_{\odot}$ black hole. We estimate that the post-explosion envelope will have $\rho_{0,He} t_0^3 \approx 1.85 \times 10^7$ ergs gm^{-1} , $\rho_0 \approx 3$ gm cm^{-3} and $t_0 \approx 0.05$ hrs. Even assuming that the flow does begin as dust-like, we find that $t_{dust} \approx 4$ hrs ($t_{crit} \approx 10$ hrs) so that the luminosity at $t \sim 60$ days will be only $\sim 5.3 \times 10^{35}$ ergs s^{-1} - a few percent of the values found above. While recombination is likely to occur earlier in such supernova, the actual accretion rate in such an explosion

will be strongly modified due to high initial temperatures (and pressure), confirming that even radioactive-free Type Ib/Ic supernovae are unlikely to be good candidates for observing the emergence of black holes.

6. CONCLUSIONS, DISCUSSION AND OBSERVATIONAL PROSPECTS

In this work we have examined the emergence of luminosity due to spherical accretion onto black holes formed in realistic supernovae. The study is based on a combination of analytic estimates and numerical simulations. Our main focus has been on SN1997D, where the low explosion energy and very low inferred abundance of ^{56}Co in its ejecta provide a possible (and currently, the only) candidate where the emergence of a black hole in a supernova may actually be observable.

We confirmed the main features of the accretion history and luminosity as derived by Zampieri et al. (1998a). At late times, the accretion flow settles on a dust-like motion, and the accretion rate falls off as a $t^{-5/3}$ in time (Colpi et al., 1996). Accretion proceeds in a sequence of quasistationary states, so the accretion luminosity achieves the expected magnitude of a hypercritical, spherical accretion flow (Blondin, 1986), accounting for the secular decay in time of the accretion rate. The resulting time dependence of the late-time accretion luminosity is $L(t) \propto t^{-25/18}$. This relation marks a fundamental feature regarding emergence: since the main competitor to accretion in powering the late time light curve is radioactive heating which decays exponentially with time, emergence of the accretion luminosity is inevitable if spherical accretion does indeed persist. While in typical Type II supernovae the abundance of radioactive isotopes is expected to be large enough to prevent a practical observation of the emergence, more rare explosions where this abundance is significantly reduced and fallback is enhanced provide important exceptions.

The case of SN1997D offers a unique opportunity to examine black hole emergence (Zampieri et al., 1998b), in view of its inferred explosion energy of $\sim 4 \times 10^{50}$ ergs s^{-1} and very low abundance of ^{56}Co , i.e., only $2 \times 10^{-3} M_{\odot}$ (Turatto et al., 1998; Benetti et al., 2000). We have examined the expected emergence of a black hole in SN1997D analytically and numerically. In the analytic study we noted that the early-time accretion is almost certain to generate an Eddington-rate luminosity, which will modify the accretion history and decrease the late-time accretion rate. In the numerical investigation we have included the effects of a variable envelope composition. In particular, we incorporated heating due to radioactive decays, including a finite (time-dependent) γ -ray optical depth. The wide diversity of time scales involved compelled us to use a rescaling scheme in the numerical simulations (see in the appendix).

Our various analyses offer a consistent assessment of the emergence of the black hole in SN1997D. We confirm the preliminary estimate of Zampieri et al. (1998b) that a $3 M_{\odot}$ should emerge in SN1997D about 1000 days after the explosion, in contrast to hundreds of years in the case of “standard” Type II supernovae (like SN1987A) where the abundances of radioactive elements are significantly higher. We show that the dominant parameter in determining the luminosity at emergence is the amount of kinetic energy carried in the post-explosion helium-rich layer (which is the source of late-time accretion). For realistic values of this energy, we estimate that the total luminosity at emergence will lie in the range $5 \times 10^{35} \lesssim L_{tot} \lesssim 3 \times 10^{36}$ ergs s^{-1} , emerging at 1000–1500 days after the explosion. In our numerical study we have examined the best fit model of Turatto et al. (1998)

for SN1997D. The simulations suggest that, for this particular model, the black hole emerges at about 1050 days after the explosion, with $L_{tot} \approx 6.5 \times 10^{35}$ ergs s^{-1} . The results of the simulation, which is based on a consistent, fully-relativistic, radiation-hydrodynamics code, provides significant support to the analytic approach. Most notably, it demonstrates that, after passing through an early radiation-pressure-limited stage which reduces the accretion rate, the accretion flow does settle on the dust-like solution and that the influence of the radioactive decays on the hydrodynamic evolution is negligible for the low abundances inferred in SN1997D.

The time of emergence and the corresponding luminosity depend on the abundances of ^{57}Co and ^{44}Ti in the envelope, which are unknown a-priori. However, as long as the accretion luminosity is significantly larger than the threshold set by positron emission in ^{44}Ti decays, both emergence time and luminosity will not vary substantially. At the time of emergence γ -ray escape from the envelope is non-negligible and increases rather rapidly with time, as the envelope's optical depth drops. Correspondingly, the bolometric luminosity due to radioactive heating decreases even faster than exponentially with time.

Although our results appear to be quite robust within the context of the present study, some uncertainties arise due to effects not considered here. Most critical is the assumption of perfectly spherical accretion: if the bound material can maintain sufficient angular momentum, a centrifugal barrier would drive the flow into a disk structure (Chevalier, 1996). The radiative efficiency of hypercritical disk accretion is uncertain, complicating any a-priori estimate regarding the character of the late-time accretion luminosity. The residual angular momentum is likely to be dependent on the details of the progenitor and the explosion (we note that for SN1987A the observed neutrino burst seemed consistent with nonrotating models (Burrows, 1988), indicating that angular momentum of matter close to the collapsed core did not play a significant role). In principle, late time accretion occurs many viscous time scales after the explosion, and much of the initial angular momentum could be lost, but the minimum specific angular momentum required to force disk accretion is quite small (about $(GM_{BH}R_{ISCO})^{1/2}$, where $R_{ISCO} = 6GM/c^2$ is the innermost-stable circular orbit near a black hole). Furthermore, even if at late times angular momentum is negligible, some residual effect may arise if the character of the early-time accretion has been sufficiently altered (Mineshige et al. 1997 found through simulations that sufficient angular momentum strongly affects the magnitude and time dependence of the accretion during the first *hours* after collapse). We defer further investigation of fallback including angular momentum to future work.

Additional effects could arise due to convection, mixing and clumping of envelope material (and radioactive isotopes in particular), and dust extinction, although we expect that at a time of $\gtrsim 3$ years after the explosion, any dust formed will have become transparent to the underlying luminosity. This may not be true if photoionization by the central accreting black hole (not included in our calculation) is important.

Our results illuminate the uniqueness of SN1997D. It is the low abundance of radioactive elements, combined with the low explosion energy in general, that allows the black hole to emerge only a few years after the explosion, at which time the absolute magnitude of the accretion luminosity is still quite large (recall that for “standard” explosions we expect emergence luminosities of $10^{32} - 10^{33}$ ergs s^{-1}). Since gas and radiation are in LTE in the inner accreting region and the pho-

tosphere is well localized in radius, the emerging spectrum is expected to be very similar to a blackbody at the photospheric temperature (~ 7500 K) with the superposition of heavy line elements. We therefore expect that emission will be mainly in the optical band. At a distance of ~ 14 Mpc, the corresponding apparent magnitude for the range of emergence luminosities predicted for SN1997D is $m_V \approx 28 - 30$ and $m_R \sim m_I \approx 27 - 29$. The higher luminosity (lower magnitude) end of this range coincides with the detection threshold of the HST STIS camera, indeed making emergence in SN1997D potentially *observable*. We note that the capabilities of HST are needed both because of the faintness of the source at this time, and the resolution, required to distinguish the supernova over the background of the parent galaxy NGC 1536. A recent estimate (M. Turatto 1999, private communication) suggests that the required exposure time for the HST STIS to resolve the apparent magnitude expected at emergence in SN1997D at a signal to noise (S/N) ratio of 10 would be ~ 25000 seconds. The accretion luminosity should be distinguishable from radioactive heating (or from circumstellar interaction, which has not been observed in SN1997D so far, Benetti et al. 2000) due to its unique power law dependence. This would be especially true if the abundances of ^{57}Co and ^{44}Ti are negligible, since after emergence the luminosity would be due only to accretion. But, even if there is a finite contribution from these two isotopes to the light curve, the presence of a power-law source may still be identifiable if several measurements with reasonable accuracy could be made. The novel consequences of a positive observation are self-evident - the first *direct* observational evidence that a black hole can be formed by an otherwise “successful” supernova. Although our main focus has been SN1997D, other theoretical Type II supernova models offer more favorable conditions for an actual observation of black hole emergence. The survey of Woosley & Weaver (1995) suggests that progenitors with masses in range $30 - 40 M_{\odot}$ are quite likely to leave behind a remnant of mass $3 - 10 M_{\odot}$ and a practically radioactive-free envelope, as all the iron group isotopes are engulfed by the early fallback. Our calculations in § 5 show that accretion luminosity will emerge after recombination depletes the initial internal energy of the envelope, hence after *a few tens of days*. The corresponding luminosity at emergence will be $\sim 10^{37}$ ergs s^{-1} , which with the present capabilities of HST would allow for detection at emergence perhaps out to $20 - 25$ Mpc. The luminosity at emergence is higher than for SN1997D so that the galactic background would be less important, and ground based instruments might be relevant as well.

How often can we expect an opportunity to observe a black hole emerging in a supernova? An upper limit is, of course, the rate at which black hole forming supernovae occur. Adopting the recent results of Fryer & Kalogera (1999) that about 10% of core collapse supernovae make black holes, we expect a rate of about one event per thousand years per galaxy. There are somewhat less than one thousand galaxies at a distance $\lesssim 20$ Mpc from the Milky way, and hence there may be approximately one observable event (equal or better than SN1997D) per several years. This estimate is an upper limit, since a significant fraction of high mass progenitors will end their lives as Type Ib/Ic supernovae after losing their hydrogen envelope, and such supernovae are unfavorable for a practical observation at emergence. Furthermore, even “perfect” candidates may not allow for an actual observation, as seems to have been the case in SN1994W. Following its recombination peak, the tail of the SN1994W light curve failed to settle on an exponential decay

that would arise due to ^{56}Co decay (Sollerman et al., 1998). Interestingly, the last data point led to a limit of $\leq 2 \times 10^{-3}$ on the mass of ^{56}Co in the ejected envelope. However, the light curve showed a very steep power-law in time until it dropped below the detection threshold some 220 days after the explosion. The luminosity during this phase was much too high to be due to accretion ($10^{40} - 10^{42}$ ergs s^{-1}) and Sollerman et al. (1998) found that it was most likely caused by interaction with circumstellar material, with dust formation also playing an important role. We can only speculate that in the absence of circumstellar interaction and dust extinction, the light curve would have declined exponentially after the recombination peak and the accretion luminosity may have emerged while still marginally detectable. The case of SN1994W implies that the rate of potential observable black hole emergence may be significantly smaller than that of black hole forming Type II supernovae.

Nonetheless, we urge that any Type II supernovae which

shows a diminished ^{56}Co abundance should be monitored, and its light curve be tracked for several months after the explosion. The prospects of observing black hole emergence may improve significantly with potential future instruments, such as NGST or a dedicated faint-supernovae project.

We are grateful to Tim Young for providing us with the results of early-time simulations for SN1997D and to Chris Fryer, Robert Kirshner, Phillip Pinto and Massimo Turatto for useful discussions. We thank Monica Colpi and Roberto Turolla for carefully reading the manuscript. This work was supported by NSF Grants AST 96-18524 and PHY 99-02833, and NASA Grants NAG 5-7152 and NAG 5-8418 at the University of Illinois at Urbana-Champaign. L. Z. acknowledges financial support from the Italian Ministry for University and Scientific Research (MURST) under grant cofin-98-2.11.03.07 at the University of Padova.

APPENDIX

THE RESCALING SCHEME: RADIATION-HYDRODYNAMIC RENORMALIZATION

The inclusion of the accreting region imposes an inherent obstacle in any numerical simulation of a supernova light curve. In the innermost accreting region the material is free-falling at a velocity which is a significant fraction of the speed of light, so that the dynamical time scale is less than 10^{-3} sec. On the other hand, the evolutionary time for the light curve is of the order of tens of days to clear the recombination phase, and years to reach black hole emergence if there is a non-negligible amount of radioactive elements in the envelope. This extreme diversity of time scales prevents any single calculation which tracks the entire envelope.

As described by Zampieri et al. (1998a), a considerable increase in the shortest physical time scale (and, hence, the Courant integration time step) can be obtained moving the inner boundary, R_{in} , outward (at hundreds to thousands of Schwarzschild radii, but always *well within* the accreting region). This turns out to be possible because the gas in the inner accreting region is in LTE and in free-fall, thus allowing a reliable setting of the boundary conditions even if R_{in} is much larger than the black hole horizon. When a Lagrangian zone passes through the inner boundary, it is removed from the calculation and the remainder of the envelope quantities are rezoned to maintain a satisfactory resolution.

Even with such a relocation of the inner boundary, the feasibility of a numerical computation requires some additional measures to accelerate the computation. To this end, the code incorporates the Multi-Time-Step Procedure, where the integration domain is separated into several subgrids, and each is evolved at its own local time scale; most of the CPU time is thus devoted to evolving the regions with smaller time steps. We note that this procedure requires a communication scheme between the sub-grids based on extrapolation, and can be safely used when there are no sharp features propagating through the envelope. Thus, we use it only after that the recombination front has completed its sweep of the envelope material. The speed-up allowed by the MTP is typically a factor of 5-8.

Unfortunately, moving the inner boundary outward and using the MTP is not sufficient when the target physical time is of the order of years⁹. In the case of SN1997D, tracking the evolution of the envelope for ~ 1000 days would require roughly 1000 CPU hours on the SGI 500MHz EV6 compaq XP1000 processor which we have used for the simulations. We were hence compelled to develop an additional acceleration algorithm, which is a rescaling scheme that allows us to integrate to the black hole emergence stage within a reasonable computational time.

Principles of Rescaling

The main objective in devising a rescaled model of a specific supernova evolution is to maintain all the quantitative features of the realistic model, while reducing the required computational time. The code uses an explicit Lagrangian scheme. Since the photon transport is treated by actually solving the transport equation, the reference velocity is the speed of light, and the Courant time step is determined by the width of the thinnest zone. This is always the innermost zone, $\Delta R_{in}(t)$, which at any time t is a given fraction of the position of the inner boundary, $R_{in}(t)$. The efficiency of the code is essentially determined by comparing the (small) ratio of the time step to a characteristic evolutionary time – for example, the expansion time scale, t_0 –

$$\frac{\Delta R_{in}(t)/c}{t_0} \propto \frac{R_{in}(t)/c}{t_0}. \quad (\text{A1})$$

The essence of a rescaling scheme would then be devising a rescaled model where

$$\frac{R_{in}^s(t^s)/c}{t_0^s} = \alpha \frac{R_{in}(t)/c}{t_0}, \quad (\text{A2})$$

⁹We note that using a fully implicit code would not allow a significant gain in computational time because limitations on the time-step imposed by accuracy are comparable to limitations imposed by the Courant condition throughout most of the evolution.

where a subscript s denotes the rescaled quantities. The rescaled model is then more efficient by a factor of $\alpha > 1$.

Successful rescaling must (a) provide a simple relation between its own physical quantities and that of the realistic model and (b) maintain the hierarchy (inequalities) of time and energy scales that exists in the realistic model, so that the relative importance of the different physical process is carried on into the rescaled model. The rescaling scheme we have chosen to employ in our simulations is detailed below.

The Rescaling Relations

A natural rescaling scheme would be one where all the physical quantities of a mass element (r, v, T, ρ, \dots) of the realistic model are mapped with simple linear relations to the rescaled model, i.e., $r^s = \alpha_R r$, $v^s = \alpha_V v$, etc. In our rescaling scheme we distinguish between the local thermodynamic and kinematic quantities of the mass elements in the envelope. Since the photon opacities are sensitive and complex functions of the thermodynamic quantities, i.e., density and temperature, we find it preferable to leave these quantities unchanged in the course of rescaling $T^s = T$, $\rho^s = \rho$, which leads to $c_s^s = c_s$, $\kappa^s = \kappa$. Note that such a choice also implies that the inner boundary of the realistic model should approximately map onto the inner boundary in the rescaled model, since the position of the inner boundary is determined by the requirement of LTE, which arises from the local values of temperature and density.

Once this choice has been made, the constraints on the rescaling scheme are quite straight forward. If we require that the ratio of diffusion and recombination times scales to the expansion time scale remain unchanged, i.e.,

$$\frac{t_{diff}^s}{t_0^s} = \frac{t_{diff}}{t_0}, \quad \frac{t_{rec}^s}{t_0^s} = \frac{t_{rec}}{t_0}, \quad (A3)$$

the rescaled model must satisfy (see eqs. [4,6]):

$$R_0^s V_0^s = R_0 V_0. \quad (A4)$$

The condition (A4) is sufficient to determine the rescaling strategy when consistently mapping all radii between the realistic and the rescaled models. If all radii are decreased by a factor of α , all velocities must be increased by the same factor; the efficiency of the simulation (eq. [A1]) is then increased by a factor of $\alpha^{-1}/\alpha^{-2} = \alpha$.

If we further impose invariant luminosity ratios according to

$$\frac{L_{diff,0}^s}{L_{acc,0}^s} = \frac{L_{diff,0}}{L_{acc,0}}, \quad \frac{L_{rec}^s}{L_{acc,0}^s} = \frac{L_{rec}}{L_{acc,0}}, \quad (A5)$$

we arrive (using eqs. [3,7 and 19]) at the condition

$$M_{BH}^s R_0^s = M_{BH} R_0. \quad (A6)$$

The principle relations of our rescaling scheme are thus

$$\left(\frac{R_0^s}{R_0}\right)^{-1} = \left(\frac{V_0^s}{V_0}\right) = \left(\frac{M_{BH}^s}{M_{BH}}\right) = \alpha. \quad (A7)$$

This choice of rescaling allows us to consistently map the marginally bound shell of the envelope, since the marginally bound radius, R_{mb} also rescales as $R_{mb,0}^s = (2M_{BH}^s (t_0^s)^2)^{1/3} = \alpha^{-1} R_{mb,0}$.

Further relations that immediately follow are

$$\left(\frac{t^s}{t}\right) = \alpha^{-2}, \quad \left(\frac{L_{acc,0}^s}{L_{acc,0}}\right) = \alpha^{-1}, \quad \left(\frac{M_{end}^s}{M_{env}}\right) = \alpha^{-3}, \quad \left(\frac{\dot{M}^s}{\dot{M}}\right) = \alpha^{-1}. \quad (A8)$$

The efficiency of rescaling is explicit in the rescaling of time – in the rescaled model all physical times are reduced by a factor of α^2 , while the *numerical* time step is only reduced by a factor of $R_m^s/R_{in} = \alpha$.

Limitations of Rescaling

The rescaling scheme presented above is not without limitations; most notably, the acceleration factor, α is limited to a value of a few, as discussed below. Nonetheless, even a value of $\alpha = 5$, which was used in the case of SN1997D reduces the required computational time from weeks to days, hence allowing for a practical numerical investigation.

The Acceleration Factor

Since the rescaling scheme calls for an increase of a factor of α of the envelope velocities, clearly α cannot be arbitrarily large, since we must maintain a sub-relativistic envelope. Furthermore, since the black hole mass is increased, its Schwarzschild radius increases as well, and naturally it should not be allowed to approach the integration domain throughout the calculation. Both these constraints result in the practical limit on the value of α to no more than a few.

Radioactive Elements

The scaling laws of luminosity and mass in equation (A8) create an undesired inconsistency regarding the luminosity from radioactive heating, since for this source $L \propto M$. In order to recover the correct rescaled power output from radioactive decays, the energy generation rate from radioactive decays per unit mass in the envelope must therefore be increased by a factor of α^2 . This could potentially impose a significant deviation in the evolution of the rescaled model from that of the original one, if it artificially enhances the importance of energy deposition from radioactive decays when compared to the other energy scales. However, since we limit ourselves to envelopes where the abundance of radioactive elements is very small, the artificial amplification of the energy production per unit mass of radioactive decays has a negligible effect.

It is further noteworthy that the effective transparency of the photons to the γ -ray photons emitted in the decays must be adjusted in order to recover the appropriate scaling of the γ -transparency time. The simple form of γ -ray opacity (eq. [11]) allows to achieve consistency with the change $\kappa_\gamma^s = \alpha \kappa_\gamma$, so that $t_{trans,\gamma}^s/t_0^s = t_{trans,\gamma}/t_0$. A similar transformation for the optical photons would be more complex, but can be neglected since the onset of thermal-photon transparency is imposed by recombination (rather than expansion), and is chiefly determined by the thermodynamic variables ρ and T , which are kept invariant.

The Accretion Time Scale and Radius

A second inconsistency that arises in this particular rescaling scheme concerns the initial accretion time and radius, $t_{acc,0}$, $R_{acc,0}$. As is evident from equations (13, 15), when the thermodynamic properties of the helium layer are not changed, so that the sound speed is conserved, $t_{acc}, R_{acc} \propto M_{BH}$. Our rescaling scheme actually *increases* these quantities by a factor of α , while other characteristic times and radii are *decreased* by factors of α^2 and α , respectively. This is an inevitable consequence of our choice of rescaling.

This inconsistency is significant, however, only while the accretion flow is Bondi (1952)-like, when $t_{acc} \leq t_0$ and $R_{acc} \leq R_{mb}$ (Colpi et al., 1996). As the envelope continues to expand, the hierarchy of time scales and radii is eventually reversed and the accretion eventually transforms into a dust-like flow. Since the accretion time does not enter explicitly in any of the estimates for evolution and luminosity (see § 2), it is only this hierarchy which is of real consequence, and hence rescaling can be applied safely to models which are characterized by $t_{acc} \gg t_0$, $R_{acc} \gg R_{mb}$.

Kinetic vs. Thermal Energies

A similar analysis concerns the ratio of kinetic and thermal energies in the envelope. It is clear that the kinetic energy will scale as $E_{kin} \sim MV^2 \rightarrow E_{kin}^s/E_{kin} = \alpha^{-1}$, while the internal energy (neglecting radioactive heating) will scale as $E_{th} \sim R^3 \rightarrow E_{th}^s/E_{th} = \alpha^{-3}$, since the temperatures are unchanged. Rescaling thus amplifies the relative importance of kinetic energy over thermal energy in the expanding envelope.

However, as is the case for the accretion and expansion time scales, the real issue is the hierarchy of energy scales. In fact, the assumption of homologous expansion is equivalent to assumption that the conversion of thermal energy to kinetic energy is negligible, i.e., that $E_{kin} \gg E_{th}$, which is satisfied in the context of our rescaled models.

A Test of Rescaling

We demonstrate here the reliability of our rescaling scheme by studying a specific example. We assume a supernova envelope somewhat similar to the SN1997D case examined in § 4, with several simplifications that allow for a more rapid computation. The basic features of the model are presented in table A2 and in Figs. A.4-A.4. We note that the initial velocity profile throughout the entire envelope was set so that $v(r) = r/t_0$. The initial accretion time-scale is determined by the properties of the region of bound material. A single fiducial radioactive isotope was included, with a mass fraction which is 0.01 of that of oxygen. This isotope was assumed to emit all the decay energy in γ -rays.

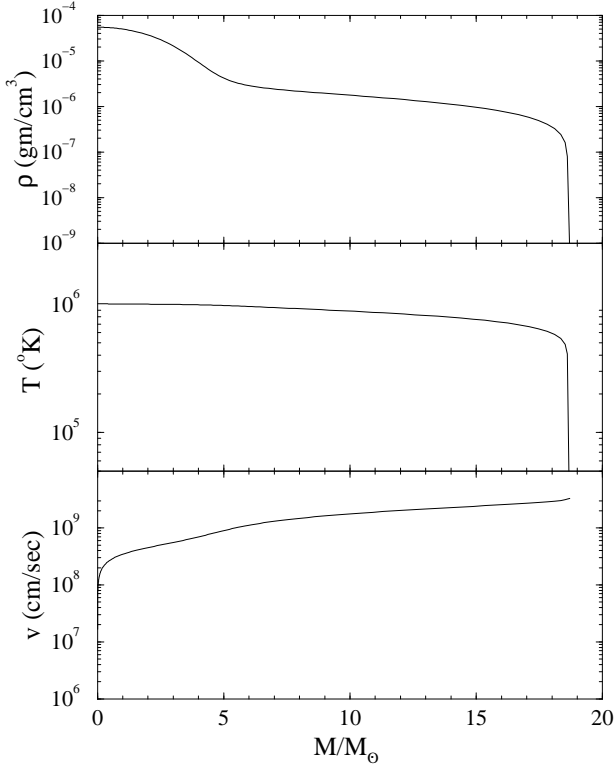


FIG. A11.— Initial profile for the toy model: density, temperature and velocity.

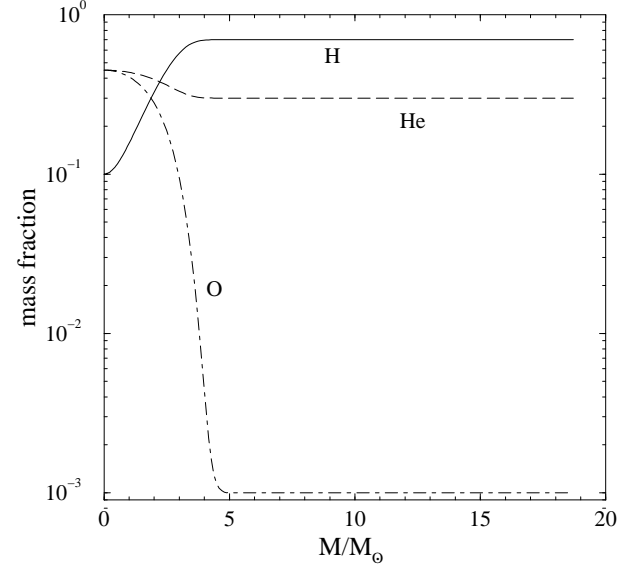


FIG. A12.— Initial profile for the toy model: composition (mass fractions of H-He-O).

We have carried out two simulations of this model, the first in its original form and once rescaled by a factor $\alpha = 5$ (since $t_0 \ll t_{acc,0}$ and $R_{mb,0} < R_{acc,0}$ to begin with, the model can be rescaled at $t = 0$). The light curves of both models are compared in Fig. A13, where luminosity and time in the rescaled model were rescaled inversely in order to compare them to the results of the original model, i.e., $L^s(t^s) \rightarrow \alpha L^s(\alpha^2 t^s)$. We note that the rescaled model required only 60 CPU hours, compared to about 300 CPU hours for the original model to reach an equivalent evolutionary stage.

TABLE A2
PARAMETERS FOR THE TOY MODEL USED TO TEST RESCALING *

model	M_{BH} (M_\odot)	M_{tot} (M_\odot)	M_{He}^a (M_\odot)	M_H^b (M_\odot)	R_{out}^c (cm)	R_{He}^d (cm)	V_{out}^e (cm s $^{-1}$)	M_{ra}^f (M_\odot)	ϵ_{ra}^g (ergs gm $^{-1}$ s $^{-1}$)	τ_{ra}^h (days)	κ_{ra}/Y_e^T i (cm 2 gm $^{-1}$)	t_0 (hrs)	$t_{acc,0}$ (hrs)
Original	3	18.75	3.75	15	2×10^{13}	4.5×10^{12}	6.67×10^8	0.036	9×10^8	50	0.01	25/3	50
Rescaled	15	0.15	0.03	0.12	4×10^{12}	9×10^{11}	3.35×10^9	2.88×10^{-4}	2.25×10^{10}	2	0.05	1/3	250

*Rescaled by a factor $\alpha = 5$ (see text)

^amass of helium-rich layer

^bmass of hydrogen rich layer

^couter radius

^douter radius of helium-rich layer

^einitial velocity at outer radius

^ftotal mass of radioactive isotope in the envelope

^genergy generation rate per unit mass of radioactive isotope

^hlife-time of radioactive isotope

ⁱ γ -ray opacity per electron radioactive isotope

The reliability of rescaling is evident from the very good agreement of the light curve and accretion rate history. In particular, the accretion luminosities at emergence agree to better than 10% (and a similar agreement is found in the accretion rates). We note that there is an obvious deviation in the light curve during the recombination phase, which is not unexpected since recombination is a non-linear process (Arnett, 1996): the rescaled model has smaller physical size, and the recombination front crosses it more quickly. This discrepancy is not important for determining the late-time accretion rate and luminosity, since the accreting region is unaffected by the recombination occurring much further out in the expanding envelope.

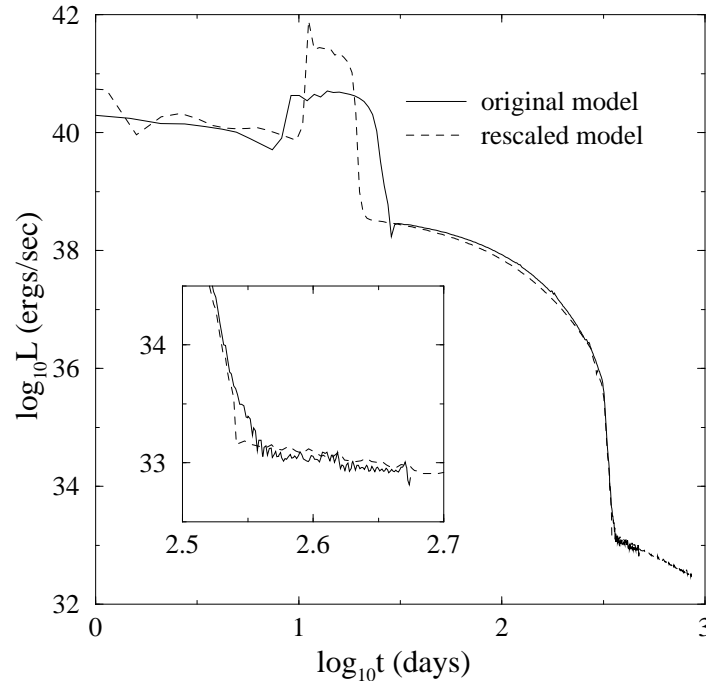


FIG. A13.— Calculated bolometric light curve of the toy model shown in Fig. A.4 (solid lines), compared with the calculated light curve of model rescaled by a factor of 5 (dashed lines). The inset shows the light curves at the time of emergence of the black hole

REFERENCES

- Alexander, D. R., & Ferguson, J. W. 1994, *ApJ*, 437, 879
 Arnett, D. 1980, *ApJ*, 237, 541
 Arnett, D. 1996, *Supernovae and Nucleosynthesis* (Princeton: Princeton University Press)
 Arnett, D., Bahcall, J. N., Kirshner, R. P., & Woosley, S. E. 1989, *ARA&A*, 27, 629
 Bethe, H. A. 1990, *Rev. Mod. Phys.* 62, 801
 Bethe, H. A., & Brown, G. E. 1995, *ApJ*, 445, L129
 Benetti S. et al. 2000, *MNRAS*, submitted
 Blondin, J. M. 1986, *ApJ*, 308, 755
 Burrows, A. 1988, *ApJ*, 334, 891
 Chevalier, R. A. 1989, *ApJ*, 346, 847
 Chevalier, R. A. 1989, *ApJ*, 459, 322
 Chugai, N. N., & Utrobin, V. P. 1999, *A&A*, 354, 557
 Colpi, M., Shapiro, S. L., & Wasserman, I. 1996, *ApJ*, 470, 1075
 Cook, G. B., Shapiro, S. L., & Teukolsky, S. A. 1994, *ApJ*, 424, 823
 De Mello, D., & Benetti, S. 1997, *IAUC* 6537
 Fryer, C. L. 1999, *ApJ*, 522, 413
 Fryer, C. L., & Kalogera, V. 1999, *ApJ*, submitted
 Fryer, C. L., Colgate, S. A., & Pinto, P. A. 1999, *ApJ*, 511, 885
 Houck, J. C., & Chevalier, R. A. 1991, *ApJ*, 376, 234
 Israelian, G., et al. 1999, *Nature*, 401, 142
 MacFadyen, A. I., Woosley S. I., & Heger, A. 1999, *ApJ*, submitted (astro-ph/9910034)
 Magee, N. H. et al. 1995, *Atomic Structure Calculations and New Los Alamos Astrophysical Opacities*, *Astronomical Society of the Pacific Conference Series* (Astrophysical Applications of Powerful New Databases, S. J. Adelman and W. L. Wiese eds.) 78, 51 <http://www.t4.lanl.gov/opacity/tops.html>
 Nobili, L., Turolla, R., & Zampieri, L. 1991, *ApJ*, 383, 250
 Nomoto, K., Shigeyama, T., Kumagai, S., Yamaoka, H., & Suzuki, T. 1994, in *Supernovae, Les Houches 1990*, eds. S. A. Bludman, R. Mochkovitch & J. Zinn-Justin (North Holland), 489.
 Patat, F., Barbon, R., Capparello, E., & Turatto, M. 1994, *A&A*, 282, 731
 Pinto, P. A., & Woosley, S. E. 1989, *Nature*, 333, 534
 Shigeyama, T., & Nomoto, K. 1990, *ApJ*, 360, 242
 Sollerman, J., Cumming, R. J., & Lundqvist, P. 1998, *ApJ*, 493, 933
 Suntzeff, N. B. 1997, in *SN1987A: Ten Years After*, ed. M. M. Phillips and N. B. Suntzeff (ASP Conference Series).
 Timmes, F. X., Woosley, S. A., Hartmann, D. H., & Hoffman, R. D. 1996, *ApJ*, 464, 332
 Turatto M. et al. 1998, *ApJ*, 498, L129
 Woosley, S. E. 1988, *ApJ*, 330, 218
 Woosley, S. E., & Weaver, T. A. 1995, *ApJS*, 101, 181
 Woosley, S. E., Pinto, P. A., & Hartmann, D. 1989, *ApJ*, 346, 395
 Woosley, S. E., & Timmes, F. X. 1996, *Nucl. Phys. A*, 606, 137
 Young, T. R., & Branch, D. 1989, *ApJ*, 342, L79
 Young T. R., Nomoto, K., Mazalli, P. A., Iwamoto, K., & Turatto, M. 1998, in *Origin of Matter and Evolution of Galaxies '97*, ed. N. Kubono, (World Scientific),
 Zampieri, L., Miller, J.C., & Turolla, R. 1996, *MNRAS*, 281, 1183
 Zampieri, L., Colpi, M., Shapiro, S. L., & Wasserman, I. 1998a, *ApJ*, 505, 876
 Zampieri, L., Shapiro, S. L., & Colpi, M. 1998b, *ApJ*, 502, L149